DAM BREACH INUNDATION ANALYSIS FOR GIDABO DAM

BY
WUBALEM TOLOSA LEMA

A THESIS SUBMITTED AND PRESENTED
TO
ADDIS ABABA SCIENCE & TECHNOLOGY UNIVERSITY
COLLEGE OF ARCHITECTURE AND CIVIL ENGINEERING
SCHOOL OF POST GRADUATE STUDIES

IN PARTIAL FULFILLMENT OF THE REQUIREMENT FOR DEGREE OF MASTER OF SCIENCE IN CIVIL ENGINEERING

SPECIALIZATION: HYDRAULIC ENGINEERING

FEBURARY, 2018

ADDIS ABABA, ETHIOPIA

CERTIFICATION

I, the undersigned, certify that I read and hear by recommend for acceptance by Addis Ababa Science & Technology University a dissertation entitled "***Dam Breach Inundation Analysis for Gidabo Dam***" in partial fulfillment of the requirement for the degree of Master of Science in Hydraulic Engineering.

____

Dr. Mesay Daniel

Principal Advisor

DECLARATION AND COPY RIGHT

Wubalem Tolosa Lema, declare that this thesis is my own original work that has not been presented and will not be presented by me to any other University for similar or any other degree award.

____

Signature

ACKNOWLEDGEMENT

I hereby take opportunity to give my sincere thanks to my advisor Dr. Messay Daniel for his guidance and support in this research. Likewise, I truly thank Dr. Assefa Kebede for reviewing the final draft and his valuable feedback. I would also like to thank my friend Gizaw Mamo for his encouragement, moral support and true friendship.

ABSTRACT

Dam provides many benefits for the society, but floods resulting from the failure of constructed dams have also produced some of the most devastating disasters. The failure consequence is usually rapid downstream flood inundation which is catastrophic to life and property. In such occasions there is often little that can be done to mitigate the magnitude of the downstream flood that will typically occur and its associated damages. Dam failure analysis was performed to study the flooding risks of Gidabo dam on the downstream settlement area due to a possible failure. The Dam is located in the border area between the Oromia state and South nation, nationalities and people regional state, near Dilla, Southern Ethiopia. The study was aimed particularly to estimate the dam breach parameters, identify potential risks, determine safe settlement areas and determine preliminary alignment of flood protection work. The study was carried out in four steps. First, the breaching mode was analyzed, the critical hydrological event was identified, and four breach parameter estimators were analyzed, accordingly, breach width of 97m, side slopes 1V: 0.7H, and breach formation time of 2.6 hours were obtained. Second, a numerical simulation of the dam break flood was performed using HEC-RAS 2D modeling. Third, based on flood simulations, flood hazard risk analysis was conducted and the results indicate that the peak discharge would be 8715.1m^3/s at the breach and 8622.8 m^3/s near settlement area, located at 2.6km from the dam axis. The duration from the beginning of the dam break to the arrival of peak discharge at settlement area is 2.68 hour. The maximum depth of water reaches up to 9m. The flood map was generated to identify people already at risk and safe settlement areas; as a result, totally, 81% of the residential would be flooded. Finally, a preliminary alignment of structural flood protection dike was identified with a length of 1.25km and an average height of 15.5m that would make 98% of the settlement area on the left bank safe.

Key words: Dam-breach-analysis, breach parameters, HEC-RAS 2D modeling, Gidabo Dam, Risk analysis.

TABLE OF CONTENTS

LIST OF FIGURES

LIST OF APPENDICES

ABBREVIATIONS

2D: 2-Dimensional

USACE: United States Army corps of Engineering

HEC-RAS: Hydraulic Engineering Center for River Analysis System

SNNPRS: Southern Nations Nationalities and People Regional State

V: Vertical

H: Horizontal

FERC: Federal Emergency Regulator Commission

BFF: Breach Formation Factor

h_w: Height of water at the initiation of breach

V_{er}: Volume Eroded

$V_{w:}$ Volume of water (stored)

h_b: Final breach height

$B_{f:}$ Final Breach Width

z_3: Vertical And Horizontal Slope Summation

Bavg: Average Breach Width

MLM: MacDonald and Langridge-Monopolis

T_f: Breach Formation Time

G: Acceleration due to Gravity

F95: Froehlich (1995)

F08: Froehlich (2008)

B: Offset Factor

VGT: Von Thun and Gillette (1990)

LiDAR: Light Detection and Ranging

DEM: Digital Elevation Model

USGS: United States Geological Survey

ArcGIS: Geographic Information System

PMF: Probable Maximum Flood

ABBREVIATIONS

WWDSE: Water Works Design and Supervision Enterprise

UB: Upstream Boundary

DS: Downstream

WSE: Water Surface Elevation

1. Introduction

Dams provide beneficial functions such as flood control, hydropower, irrigation, recreation, and storage of water supplies, but they also entail risk of flooding. substantial property damage and loss of life will be the result if they breach (Shivers et al., 2015). Despite the fact that dams are presumed to serve for extended periods, there is still a possibility for failure.

In the rare event of a dam failure, there is often little that can be done to mitigate the magnitude of the downstream flood that will typically occur. The volume of water involved, particularly where a larger dam is involved, is so great that it devastates existing flood control or river control structures downstream of the dam. The mere presence of floodwaters will certainly cause water related damage in many areas, and the high velocity of flow that will likely accompany such a flood event may also cause structural or erosion related damage.

For instance, In Spain 1997, failure of a dam on the Guadalquivir River, not far from Sevilla, caused immense ecological damage from the release of polluted sediments into the river valley. More recently, in May 1999, a dam failed in Southern Germany causing 4 deaths and over 1 billion Euro of damage. In year 2005, the failure of Nand Gavan dam in Maharashtra and Pratapura dam in Gujarat caused severe flooding in downstream area. These instances of dam failures establish that hazard posed by dams, large and small alike, is very real. As public awareness of these potential hazards grows, and tolerance of catastrophic environmental impact and loss of life reduces, managing and minimizing the risk from individual structures is becoming an essential requirement rather than a management option.

Detailed knowledge, both spatially and temporally, of the floodwaters extent, the depths to which the floodwaters may reach, and the flow velocities associated with the flood can be valuable pieces of information that will enhance preparedness planning for such an event. It also helps land use planners to identify flood zones and to put into consideration while developing the area.

The emphasis of this research is to study the flooding impacts of Gidabo dam on the downstream areas through simulation of hypothetical failure. It particularly aims to estimate the dam breach parameters, identify potential risks, determine safe settlement areas, and determine preliminary alignment of flood protection work.

1.1. Statement of the problem

Gidabo dam is an earthfill embankment dam with central core. At normal water level, it has a storage capacity of more than 68 Million Cubic Meter. It is located in the Abaya sub-basin of the Rift Valley. The lake basin is found in the southern part of the country within Oromia and SNNPR States and the dam site is approachable from Addis Ababa via Dilla town. It is mainly constructed for irrigation purpose. A total of 27043ha of land is aimed to be irrigated.

The river Gidabo is main contributor to Lake Abaya. The river periodically inundates about 6000 ha land and creates temporary swamps. The surrounding of the swamp area is a habitat for Guji people. Currently, approximately 240 residential are counted on high resolution image in which 4-6 households are available in each as depicted from an interview. In addition, 20-20000 cattle including goats and sheep are owned by a single family.

Future risk of impact from the dam failure is expected to increase as population growth due to improved job opportunity in the area due to the existence of the dam. As shown in the historical image (**Error! Reference source not found.**) adopted from Google earth, it could be seen that more settlers are taking up the area downstream of the dam from time to time. This shows that the human population and resources vulnerable to risk of flooding is increasing.

It is also pertinent to mention that the area has high development opportunity. Housing will also be developed to accommodate the work force which will be required to manage the intended irrigation land. Huge investments could also be planned and constructed in these areas in relation to the produce. These will definitely raise the dam breach associated flooding risk.

Therefore, a hypothetical dam failure consequence has to be analyzed through simulation to avoid loss of life (human and animal) and structures, minimize the dam risk, and design mitigation measures or protection works.

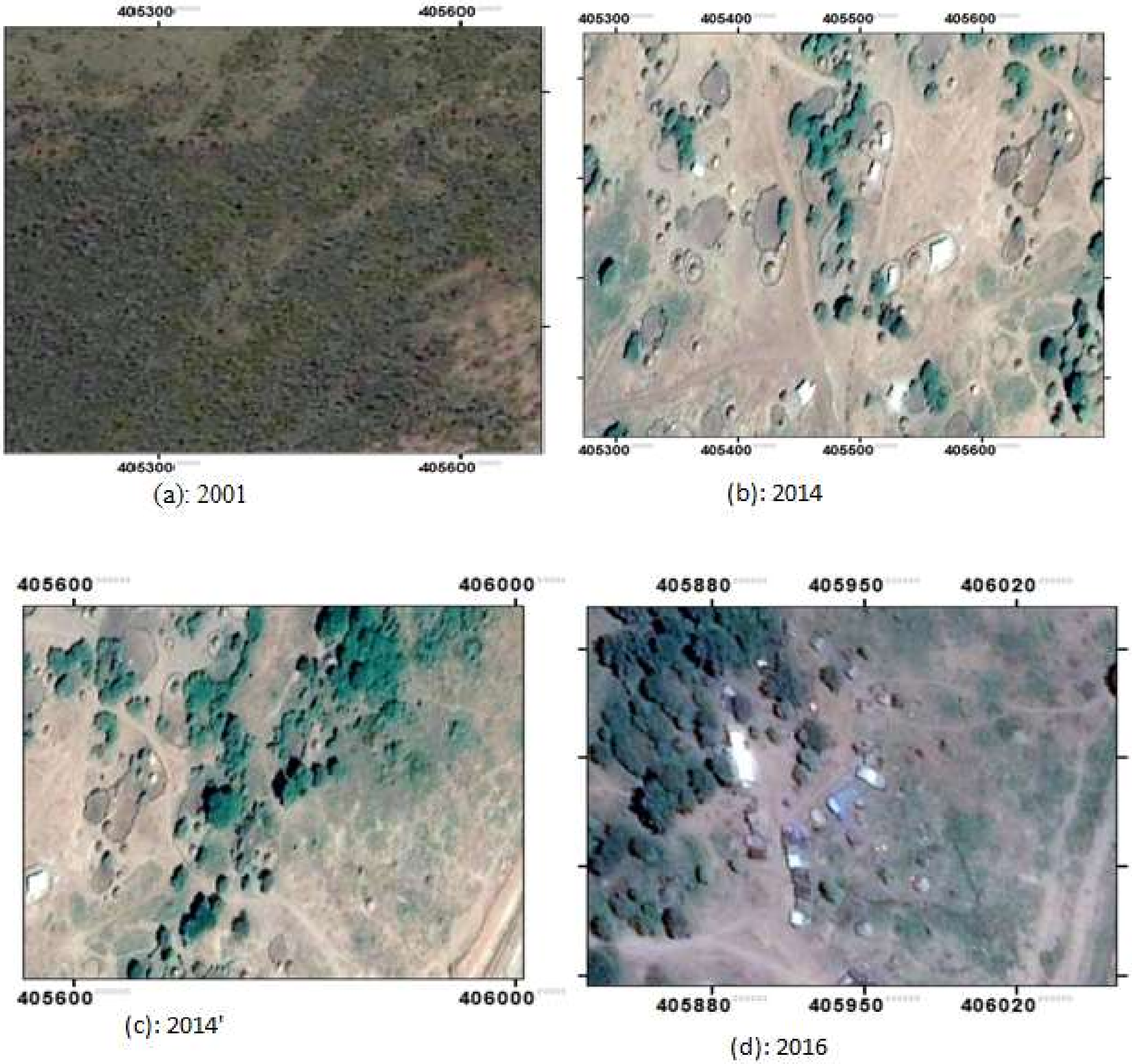

Figure 1: Downstream Area Land-use change *(source: Google earth)*

1.2. Objective

1.2.1. General Objective

The principal objective of this study is to assess the flooding impacts of Gidabo dam on the downstream settlement area due to a possible breach.

1.2.2. Specific objectives

- To estimate the dam breach parameters.
- To identify potential risks of flooding.
- To determine safe settlement areas.
- To determine preliminary alignment of flood protection work.

1.3. Research Questions

This research aimed to answer the following issues:

- How much area would be inundated in cases of a breach?
- How many life and settlers are already at risk?
- Which areas are suitable for settlement and development downstream of the dam?
- Where should flood protection be aligned so that dam risk would be minimal?

1.4. Significance of the study

Output from analysis of dam breach inundation is inundation map. The resulting flood inundation maps can provide valuable information to planners and designers, emergency managers, and local residents for planning an emergency response if a dam breach occurs. It also helps land use planners to identify flood zones and to put into consideration while developing the area.

2. Literature Review

2.1. Dam breach analysis

Dam breach analyses are used to estimate the potential hazards associated with a failure of a project structure/feature. Dam breach inundation analyses include the following elements: estimation of the dam breach parameters, estimation of the dam breach outflow hydrograph; routing of the dam breach hydrograph downstream; and estimation of downstream inundation extent and severity (FERC, 2014).

2.2. Dam risk analysis

All of the words, danger, peril, hazard, and risk, refer to an exposure to harm or loss. Because it stresses uncertainty, risk distinguishes itself from the others and is especially significant with respect to dam safety (McCuen, 2017).

The major "branches" of dam safety risk management include risk analysis, risk evaluation, and risk treatment (reduction). Risk assessment combines the first two branches and risk management combines all three. There are four major steps in a risk assessment: risk identification, risk estimation, risk evaluation, and risk treatment (consideration of reduction alternatives). Implementation of risk treatment is part of risk management (David et al., 1998).

Risk analysis involves both risk identification and risk estimation. Risk identification is the process of recognizing the plausible failure modes if the dam were subjected to each type of initiating event. Risk estimation consists of determining loading, system response and outcome probabilities, and the consequences of various dam failure scenarios and no-failure scenarios, so that incremental consequences can be estimated (David et al., 1998).

2.3. Dam breaching/failure modes

Dam failure may arise due to different reasons ranging from seepage, piping (internal erosion), overtopping due to insufficient spillway capacity and insufficient free board and to settlement due to slope slides on the upstream shells and liquefaction due to earthquakes. The documents of USACE (1997) Hydrologic Engineering Centre present the causes as follows: Earthquake; landslide; extreme storm; piping; equipment malfunction; structure damage; foundation failure; and sabotage (Xiong, 2011). Costa (1985) reports that for embankment dams only, 35% have failed due to overtopping, 38% from piping, 21% from foundation defects and 6% from other failure modes (Brunner, 2010). Overtopping failures start at the top of the dam and grow to maximum extent, while a piping failure can start at any elevation/location and grow to the maximum extents. Overtopping failure has been found to be the most crucial cause mainly with respect to time of failure; it is also the leading reason of dam failure worldwide (Ahmadisharaf et al., 2016). The most possible failure mode considered in this study was, however, piping; as there has been an experience of conduit settlement (close to 50cm) during construction. The spillway is also designed for 10,000 year or 0.5 PMF. Therefore, it is unlikely that the dam fails by overtopping.

2.4. Dam Breach Parameter Estimators

In analyzing dam breach inundations, four critical issues must be determined breach parameters (breach size/shape and time of failure), breach peak discharge and breach hydrograph estimation, breach flood routing, and estimation of the hydraulic conditions at critical locations (Kulkarni et al., 2016). Most of the dam breach parameter determination techniques are empirical equations which rely on statistical analysis through regression of data obtained from documented dam failures. MacDonald & Langridge – Monopolis (1984), Froehlich (1995), Froehlich (2008),Von Thun and Gillette (1990) and Xu and Zhang (2009) are regression equations that have been used for several dam safety studies found in the literature (Brunner, 2010).

MacDonald and Langridge-Monopolis utilized 42 data sets (predominantly earthfill, earthfill with a clay core, and rockfill) to develop a relationship for the "Breach Formation Factor." BFF is the product of the outflow volume of water and the height of the water above the breach base at time of failure (Gee, 2008). The equation series can be written as:

$$BFF = h_w * V_w \tag{1}$$

$$\text{Earthfill dams:} \quad V_{er} = 0.0261 BFF^{0.769} \tag{2}$$

$$\text{Non} - \text{Earthfill dams:} \quad V_{er} = 0.0348 BFF^{0.852} \tag{3}$$

$$T_f = 0.0179 {V_{er}}^{0.364} \tag{4}$$

$$B_f = \frac{v_{er} - {h_b}^2\left(cm + \frac{h_b m z_3}{3}\right)}{h_b\left(c + \frac{m z_3}{2}\right)} \tag{5}$$

$$B_{avg} = B_f + m h_b \tag{6}$$

Where, h_w is depth of water above breach at time of failure in meters, V_{er} is volume of embankment material eroded in cubic meters, V_w is the volume of water that passes through the breach in cubic meters and T_f is breach formation time in hours, m is breach side slope (H:V), h_b is final height of breach in meters, B_f is final breach width in meters, C is dam crest width in meters, z_3 is the summation of slope (H:V) of upstream and downstream faces of dam, and Bavg is average width of final breach in meters. MLM suggested a breach side slope of 0.5 (H:V) (Ahmadisharaf et al., 2016).

Froehlich (1995) studied 63 dam (earthen, zoned earthen, earthen with clay core and rockfill) failure events and proposed equations to estimate average breach width and formation time (Ahmadisharaf et al., 2016). The equations are as follows:

$$B_{avg} = 0.1803 K_0 {V_w}^{0.32} {h_b}^{0.19} \tag{7}$$

$$T_f = 0.00254 {V_w}^{0.53} {h_b}^{-0.9} \tag{8}$$

Where, B_{avg},h_w,h_b and V_w are the same as defined for the MLM method and K_O is overtopping coefficient, which is 1.4 for over topping and 1.0 for piping. F95 recommended a typical breach side slope value of 1.4 (H:V) for overtopping failure and 0.9 (H:V) for other types.

Froehlich (2008) studied 74 dam failure events and proposed equations to estimate time to failure and average breach width. The equation series can be written as:

$$B_{avg} = 0.27 K_0 {V_w}^{0.32} {h_b}^{0.04} \tag{9}$$

$$T_f = 0.0176 \sqrt{\frac{V_w}{g {h_b}^2}} \tag{10}$$

where, B_{avg}, V_w and h_b are the same as defined for the MLM method, g is acceleration of gravity (m/s^2) and K_0 is same as F95 but value of 1.3 is suggested for overtopping rather than the value of 1.4. F08 recommended a typical breach side slope value of 1 (H:V) for overtopping failure mode and 0.7 for other modes (Ahmadisharaf et al., 2016).

Von Thun and Gillette (1990) used 57 dams from both the Froehlich (1995) and MacDonald and Langridge-Monopolis (1984) papers to develop their methodology (Gee, 2008).
The equation series can be written as:

$$B_{avg} = B + 2.5 h_w \tag{11}$$

$$\text{Highly erodible:} \quad T_f = 0.015 h_w \tag{12}$$

$$\text{Erosion resistant:} \quad T_f = 0.020h_w + 0.25 \tag{13}$$

Where, T_f, B_{avg} and h_w are the same as defined for the MLM method and B is offset factor, which is a function of reservoir volume and can be determined based on Table 1. By using the offset factor, it accounts for reservoir volume.

Table 1:Offset factor determination in VGT Method (Ahmadisharaf et al., 2016).

Reservoir size(m^3)	B(m)
$< 1.23 \times 10^6$	6.1
$1.23 \times 10^6 - 6.17 \times 10^6$	18.3
$6.17 \times 10^6 - 1.23 \times 10^7$	42.7
$> 1.23 \times 10^7$	54.9

where, T_f, B_{avg} and h_w are the same as defined for the MLM method. VTG recommended a typical breach side slope value of 1 (H: V). Alternatively, VTG stated that slopes of 0.5 or 0.33 (H:V) may be more suited to dams with cohesive shells or very wide cohesive cores (Ahmadisharaf et al., 2016).

Xu and Zhang (2009) used 182 earth and rockfill dams from the United States and China, with nearly 50% of the dams greater than 15 meters in height. However, their final equations are based on a much smaller subset of these dams due to missing data. Their paper shows details for 75 dams that were composed of homogeneous earth fill, zoned-filled, dams with core walls, and concrete faced dams. Their final equation for the average breach width is based on 45 dam failures, and their equation for the time of failure is based on only 28 dam failures (Brunner, 2010). Xu and Zhang's regression equations are provided in Appendix-A 1and Appendix-A 2. In a nutshell, the methods predict a wide range of breach parameters and therefore, a large difference in outflow hydrographs. Gee (2008) compares all the methods to a historic estimated outflow hydrograph (Oros) and the result showed that all of the methods produced flows larger than those observed.

For analysis of hypothetical dam breach scenarios of the Pinaus Lake Dam near Vernon, BC and Cold Spring Creek Dam in Fairmont, the 1986 BC Hydro and 1993 FERC Guidelines were used to assist the fixation of breach parameters (Asnaashari et al., 2014). This guide line is provided in a table in Appendix-A 3. The assumptions regarding dam breach parameters are critical for dam break modeling. Thus, reasonable values for the breach size and development time along with feasible breach geometry are needed to make a realistic estimate of the outflow hydrographs. Nonetheless, determining the size and growth rate for breaches is an inexact science while they are key parameters in dam break models. Therefore, the estimation of the breach parameters yields a significant source of uncertainty in the results and in turn downstream inundation extent. These uncertainties require conservative assumptions to be made as a larger flood may be expected to occur and is preferred by most authorities (Asnaashari et al., 2014).Two set of breach parameters were evaluated for 11 dam failure studies. The selected model parameters for each of the dams yielding a conservative estimate of the dam breach. Most selected dam-breach parameters were within the range of the Von Thun and Gillette (1990) and Froehlich (2008) methods (Shivers et al., 2015).For this study, the methods namely: MacDonald & Langridge-Monopolis (1984), Froehlich (1995, 2008), and Xu and Zhang (2009) were applied and reasonable breach parameter estimator was adopted based on result comparison at settlement area.

2.5. Terrain data

Development of accurate flood-inundation maps requires high-resolution elevation data of known accuracy. More accurate elevation data can be used to produce more accurate flood inundation maps (Horritt and Bates, 2001). LiDAR-based DEMs represent the best source of terrain data for flood modeling due to their horizontal resolution and vertical accuracy, which is ≈0.1 m. The ability to detect bare earth as well as vegetation and building heights is also appealing (Sanders, 2007). A scale of 1:20,000 topographic map was used in representing the downstream valley from dam to the study limit (Asnaashari et al., 2014). Contour maps with a contour intervals of 6m depicting the reservoir and dam breach geometry were used after scanned, geo-referenced, and digitized using polylines in ArcGIS (Gallegos et al., 2009).Land-surface elevations were determined from a DEM created from the most detailed data sources available for the study areas. The USGS DEM with 10m horizontal resolution was used (Shivers et al., 2015).For this study a topographic map of scale 1:2000 and contour interval of 2m was used for representing the downstream flood plains.

2.6. Manning roughness coefficient

Common methods of estimating Manning's roughness coefficients for stream channels, includes use of published *n*- value data, comparison with photographs of channels for which *n* values have been computed, and *n* -value equations (Coon, 1997). A Manning *n* was assigned in accordance with a simple land cover classification that was manually created from parcel outlines and digital orthophotos, using Chow's (1995) tabular *n* values for similar land characteristics (Gallegos et al., 2009). Chow's (1959) roughness values for different land uses are provided on Appendix-A 7. channel roughness values (Manning "*n*") could also be selected based on reviewing the site visit, photographs and aerial imagery of channel and flood plain areas (Asnaashari et al., 2014). The Manning's coefficients for the channel and overbank areas have been estimated based on the field investigation (Changzhi et al., 2014). Bridges and channel roughness have substantial effects on the hydraulic properties of streams. Manning's roughness coefficients, values used to describe a channel roughness or resistance to flow was determined for the study area using methods from Rendon and others (2012), it is mainly based on photographic comparison (Shivers et al., 2015). For this study, chow's (1959) description of various flood plain land covers was used in assigning roughness value for land cover map of the study area.

2.7. Boundary conditions

Boundary conditions both at the upstream and downstream ends of the model are needed in flood routing. Their selection is dependent on the dam breach study's purpose, their locations relative to the area(s) of interest, and level of sensitivity dependent on the degree of confidence required. The upstream boundary condition can be defined by a stage-storage relationship, or as a series of cross-sections cut through the reservoir. The downstream boundary conditions points could be fixed when: there are no habitable structures, and anticipated future development in the floodplain is limited, Flood flows are contained within a large downstream reservoir, Flood flows are confined within the downstream channel, or Flood flows enter a bay or ocean (FERC, 2014). The inflow hydrographs for the upstream boundary; four extreme input hydrographs of Probable Maximum Flood (PMF), 2/3PMF, 1/3 PMF, and 1:1000 flood were considered for the flood simulations. Downstream boundary conditions were established at a large body of water. Elevation-volume tables were used to represent the storage upstream of the dams (Asnaashari et al., 2014). Upstream boundary of a normal flow hydrograph were used for piping failure (Shivers et al., 2015). For this study inflow hydrograph of 0.5 PMF, which is the design flood for the spillway, were considered as an upstream boundary. This would make the water level at the initiation of the breach at maximum (conservative level). For the downstream boundary, location away from the study area and close to Lake Abaya was considered.

2.8. Flood inundation mapping

Dam-breach flood-inundation maps indicate areas that may be flooded as a result of a dam failure. The maps are used by wide range of end-users for planning and as a response tool to determine the effects of dam failure in downstream areas. Flood inundation maps were generated using ArcGIS (Asnaashari et al., 2014).

2.9. Modeling Techniques

Generally 2D models are used in dam break modeling. In the 2D approach, there are no cross-sections, as with 1D modeling. Instead, the riverbed is defined by a network field, single grids or mesh, in which the shape can be square (cell based with regular elevation intervals) or polygonal (with irregular intervals) where each individual element has an associated elevation. The flexible mesh has an irregular representation that can be square, rectangular, triangular, or a combination of these shapes; also, the size of the shapes can vary. The Manning coefficient can be variable and applied at every element location or cell. Typical modeling software used for calculating two-dimensional flood flows includes FLO-2D, WOLF 2D, MIKE 21, TUFLOW, SOBEK, and HEC-RAS (Changzhi et al., 2014).

Model selection could be an issue when there are a lot of available numerical models. Verification and validation, handling of 2D flows, and speed are some criteria used to select one particular model (Reinaldo, 2015). Universality and usability (Changzhi et al., 2014) and modification by developers (owners) through time (FERC, 2014) are also considered in selection.

Dam failure analysis models developed by National Weather Service (NWS) such as DAMBRK, SMPDBK, and FLDWAV are widely used as well as BREACH (Xiong, 2011). Gee and Brunner (2005) compared HEC-RAS model with FLDWAV in the aspect of dam break flood routing. They concluded that the differences in the interpretation and approximation of river geometry are the primary source of the differences in the model simulations, although the numerical algorithms for solution of the St. Venant Equations or full momentum equation are similar (Xiong, 2011).

To simulate the dam-breach flood, a one-dimensional HEC-RAS model was used to simulate the dam breach process and determine breach outflow and water-surface profiles (Lejissa, 2015). HEC-RAS is the recommended tool for unsteady flow analysis as it is a free model continually being upgraded, supported by the U.S. Army Corps of Engineers, and is widely accepted as the current state-of-the-practice open channel flow hydraulic model within the civil engineering community (FERC, 2014). The continuity equation and momentum equation are the main scientific basis for unsteady flow analysis. The continuity equation is as follow:

$$\frac{\partial A}{\partial t}+\frac{\partial Q}{\partial s}-q=0 \tag{14}$$

Where, A = flow area, m^2;

Q = volume of flow, m^3/s;

q = the lateral inflow per unit length, m^2/s;

t = time variable, s;

s = spatial distance along the direction of flow, m. And one form of the momentum equation is as follow

$$\frac{\partial Q}{\partial t}+\frac{\partial QV}{\partial s}+gA\left(\frac{\partial z}{\partial s}+S_f\right)=0 \tag{15}$$

Where,

V = flow velocity, m/s;

z = elevation of water surface, m;

g = gravitational acceleration, m/s^2;

S_f = friction slope.

$$S_f=\frac{Q^2n^2}{R^{\frac{4}{3}}A^2} \tag{16}$$

Where, n = manning's roughness coefficient;

R = hydraulic radius, m

All of the 2D models mentioned above (FLO-2D, WOLF 2D, etc.) produce different results for eight cases studied. Some are closer together than others, but none are the same. There are many things that will cause different results to occur with these different models, such as: Mesh size, shape, and time step, how each model depicts the actual terrain within their mesh (Cells and faces), Friction modeling, Temporal and convective acceleration modeling, Turbulence modeling, etc. It is absolutely true that the modeler is more important than the software selected (Brunner, 2015).

2.10. Sensitivity Analysis

Like any physically based phenomena, empirical methods to predict breach geometry and timing, have uncertainty and thus influence the estimated breach outflow (Ahmadisharaf et al., 2016). Sensitivity analyses would also diminish the effect of data limitations and help to better understand the effect of the assumptions and input parameters on the extension of the inundated areas (Asnaashari et al., 2014).Sensitivity analysis is performed in order to estimate the impact of varying the model parameters to the model results. These parameters include full formation time, breach depth, breach width, and breach side slope (Changzhi et al., 2014).The water levels in the downstream inundated areas are influenced by various factors which may be put into two groups, namely the breach parameters, and the physiographic feature of the upstream basin and downstream of the dam. Though these factors are known, sensitivity tests are needed to quantify the magnitude of the effects on breach outflow and downstream water levels (Asnaashari et al., 2014). The impact of change of each breach parameter on the inundation extent was studied by increasing and decreasing the estimated breach parameters by 20% and 50% (Changzhi et al., 2014). In this study, the change in flooding extent due to changes of breach parameter was examined. Each breach parameter was increased and decreased by 20 and 50%, then the flooding risk was cheked. Hence, the worst possible floding scenario was determined.

3. Methodology

The two-dimensional dynamic (unsteady flow) modeling software Hydrologic Engineering Centers River Analysis System (HEC–RAS) was used to analyze the downstream consequences of hypothetical dam failure. Reservoir and dam profile data, terrain data, Manning's roughness coefficients, breaching parameters (breach height, width, formation time and slope) and flow and boundary conditions were required for model development. The required data were obtained from both secondary and primary sources. Most commonly used Empirical equations: MacDonald & Langridge-Monopolis(1984), Froehlich (1995,2008), and Xu and Zhang (2009) were implemented to determine breach parameters. Smart GIS was used to generate High resolution rectified image from Google earth to determine the landcover of the study area. The simulated flood was overlaid on high resolution rectified image on GIS environment for inundation mapping.

3.1. Study Area Description

3.1.1. Location

The project area is located in the Abaya-Chamo sub-basin of the Rift Valley Lakes Basin situated in the southern part of Ethiopia, within the administrative Regions of SNNPR. To be more specific, it falls in Abaya district of Borena zone Of Oromia region and Dale district of Sidama zone of SNNPRS (near Dilla town to East of Lake Abaya).

The project area lies in the low lands, very close to the Dure and Gola marsh. It lies approximately between 6°20' and 6°25' N Latitude and 38°05' and 38°10' E Longitude (Figure3. 1) a short distance to the east of Lake Abaya and just south of Gidabo river flood plain; at an average elevation of 1190 m.a.s.l.

3.1.2. Climate

The study area falls within the traditional Kola agro-climatic zone, which can be classified as semi-arid climate. The climatic data are recorded from the four observation stations – Amaro-Kelo, Bilate, Dilla and Hagere-maryam located nearby the project area. The average minimum temperature varies between 10.24^{0}C in December to 12.32^{0}C in July and the maximum temperature ranges from 25.88^{0}C to 30.52^{0}C in February. The average annual rainfall recorded so far in the project command is 1303mm with minimum of 34.9 mm in January and maximum of 208.3 mm in April. The mean monthly sunshine hours varies from 3.3 hours/day in July to 7.71 hours/day in January. The mean monthly relative humidity varies between 56.19% in February to 80.33% in September. The average wind speed varies from 0.39 m/s in July to 0.7 m/s in March. The daily estimated reference evapo-transpiration values ranges from 2.96 mm in July to 4.62 mm in March.

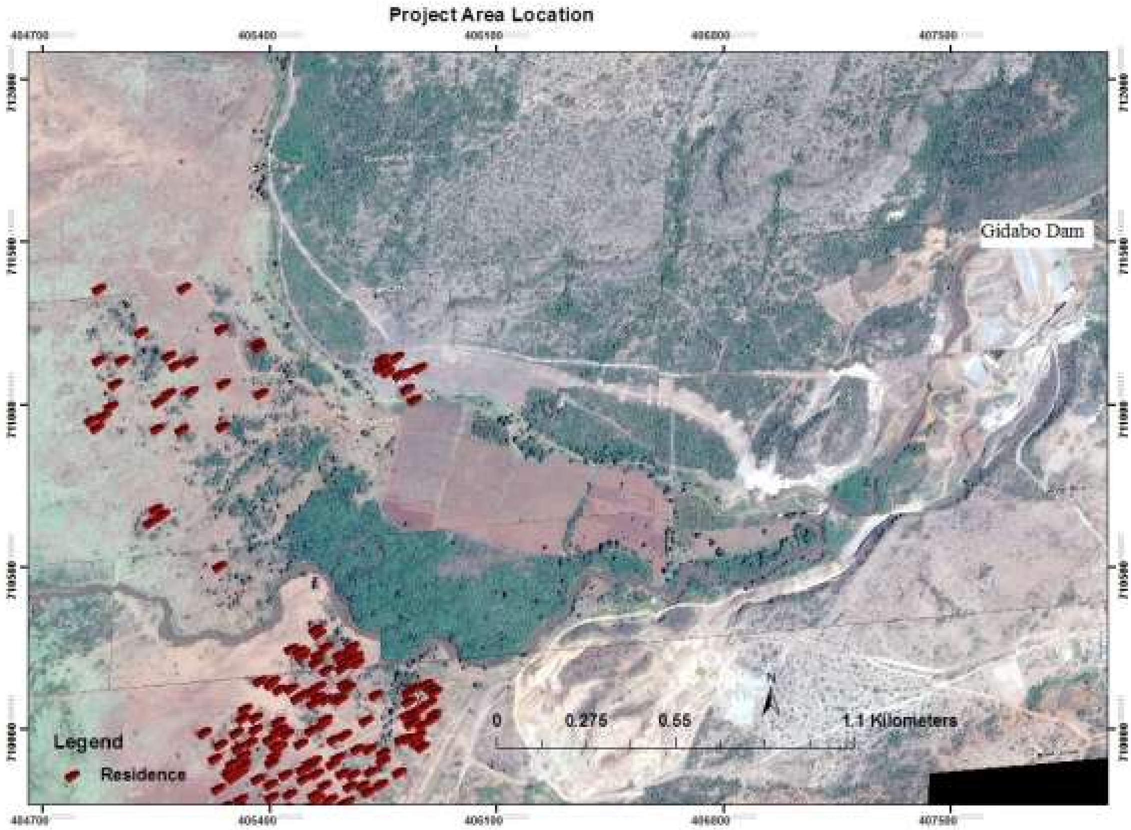

Figure3. 1: Rectified high resolution image of study area

3.2. Data

3.2.1. Reservoir data

Reservoir data were obtained mainly from drawing Albums of a design document and measurement constructed structures. The key components of Gidabo Reservoir consist of an earth fill dam with an average upstream slope of 1V:2.73H and downstream slope of 1V:3H; and impervious core of slope 1V:0.5H on both sides. The dam profile is provided in Appendix-A 4. The clay core earth dam is 26.3 m high, 345m long, 8m in crest-width with the crest elevation at 1226.3 m. The upstream and downstream faces are protected by riprap, with 8m and 5m width of berms are provided at the elevations of 1212.1 m and 1214.5m, respectively. The high flood level of the reservoir is 1223.8m; the normal water level is 1219.5 m. Figure3. 2 show storage area elevation relationship of the Gidabo reservoir. Labyrinth type of spillway with a total crest length of 75m crest is designed for 10,000 year flood. It has discharging capacity of 1391.94m^3/s. one circular outlet conduit of 1.6m is provided with upstream invert level of 1204.95m; and downstream invert level of 1204.85m.

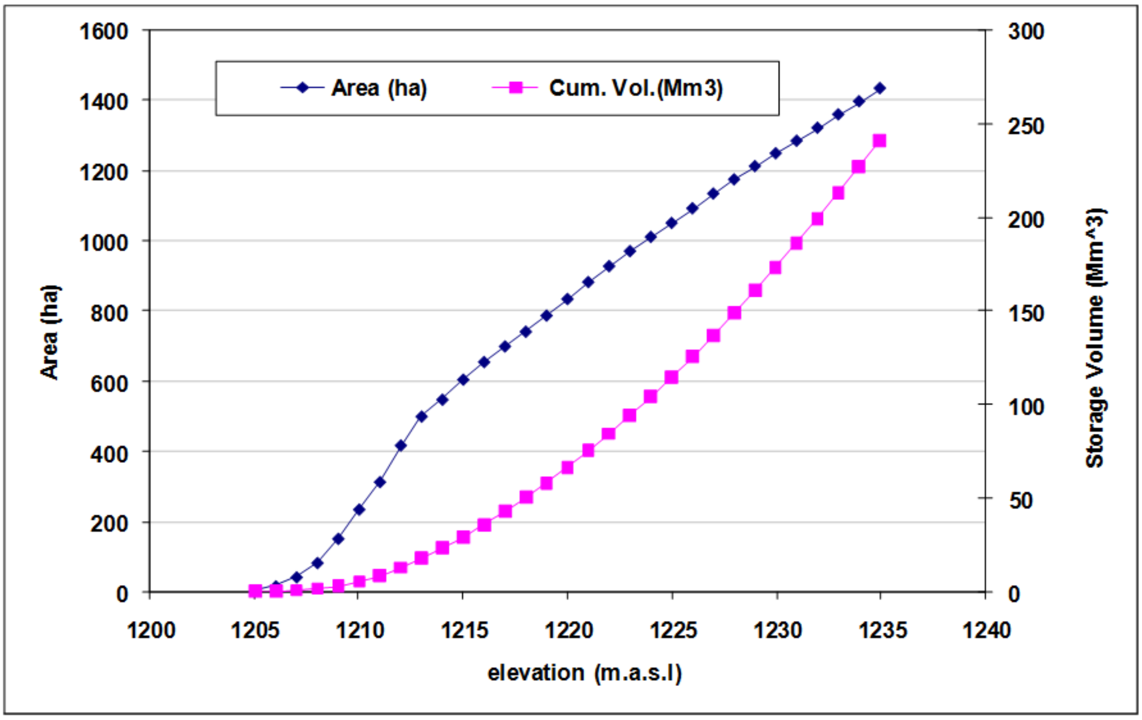

Figure3. 2: Storage –area- elevation curve *(source: WWDSE)*

3.2.2. Terrain Data

Land-surface elevations for the modeled area were determined from two sources. For most of the downstream areas a topographic map with 2m interval were used. The topographic map was obtained from Water Works Design and Supervision Enterprise (WWDSE) shown in Figure3. 3. However, for part of the upstream storage area 30m DEM from USGS website was used in combination (Figure3. 4).

3.2.3. Hydraulic Data

Manning's roughness coefficient values used to describe a channel and bank roughness or resistance to flow were determined using methods from Chow (1959). In this method, as mentioned in the literature review section 2.6 and in Appendix-A 7: manning's value for different land covers in the study area is assigned based on photographic comparisons and tabulated flood bank description.

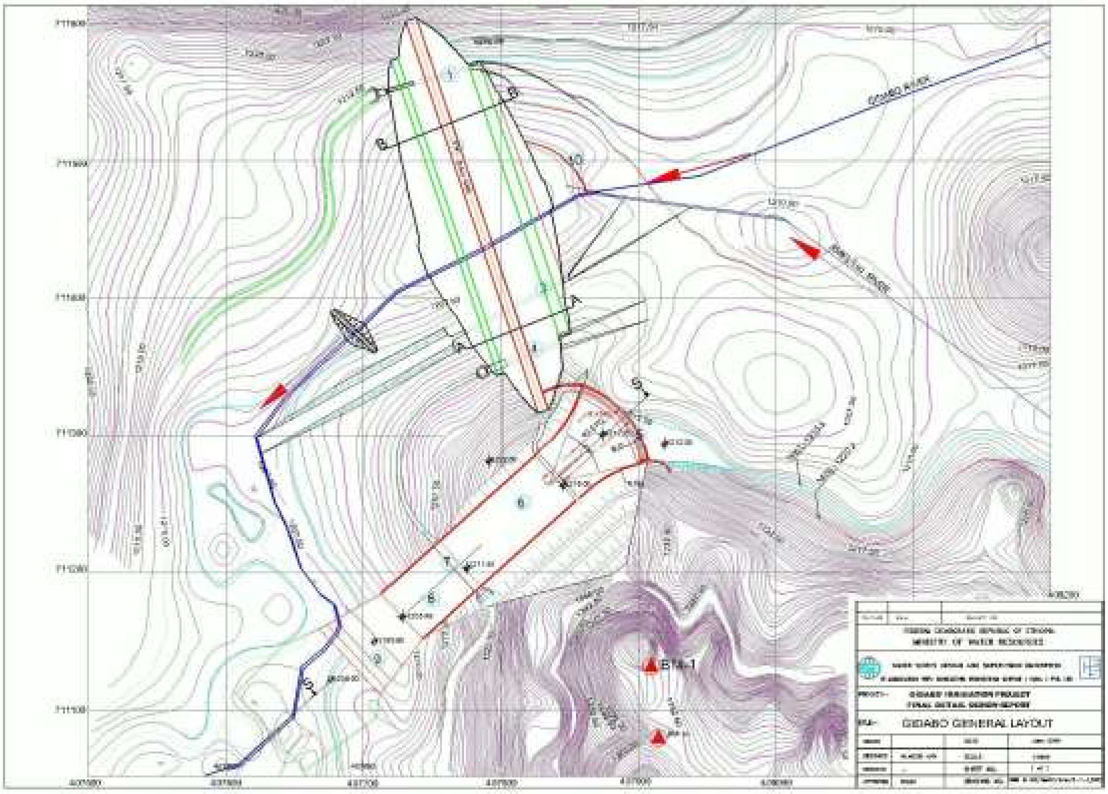

Figure3. 3: Topographic map together with the dam layout *(source: WWDSE)*

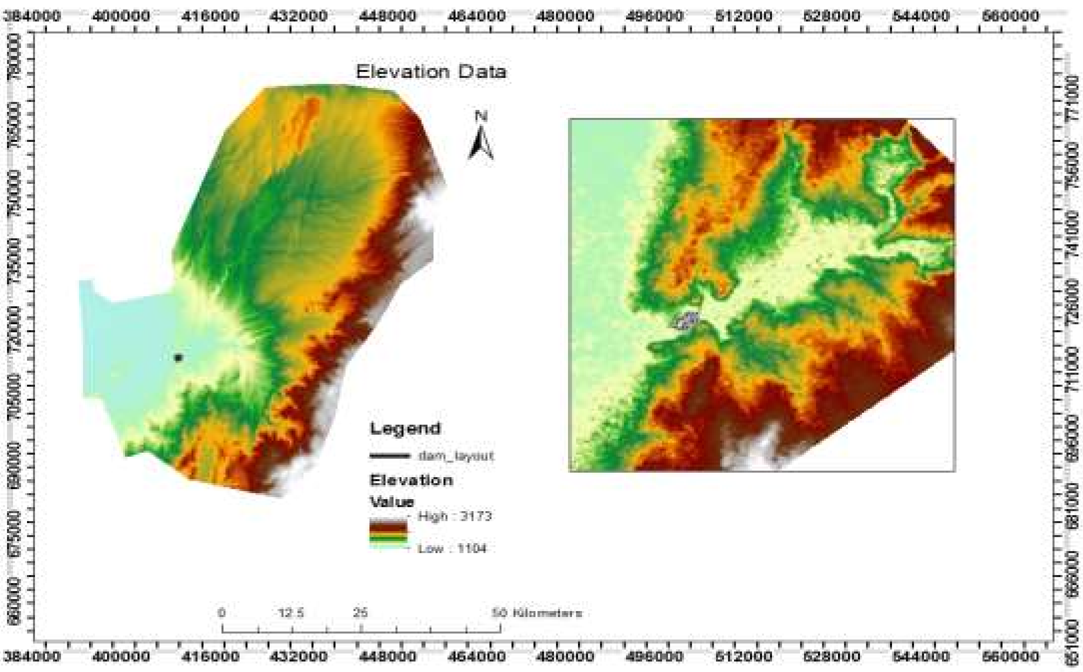

Figure3. 4: Terrain data *(source: USGS, 2011)*

3.2.4. Hydrologic Data

Flow data at the dam axis for different return periods were determined for spillway sizing and optimizing the reservoir operation by Water Works Design and Supervision Enterprise (WWDSE) in association with Consulting Engineering Services (India). This was used as a secondary data. Flow hydrograph at required cross sections (boundaries) were determined using simple area ratio technique, Based on the catchment Area. The flow hydrograph developed through frequency analysis for different return periods is shown in Appendix-A 8.

3.3. Modeling Technique

The two-dimensional dynamic (unsteady-flow) modeling software HEC–RAS was used to simulate the hypothetical breach of the dam and its propagation in the downstream. As briefly mentioned in the literature review section 2.9; verification and validation, handling of 2D flows, speed, availability, universality, and modification by developers (owners) through time are some criteria used to select a particular model. Therefore, HEC-RAS was opt as it is verified and validated for a number of cases, freely available, both one/two dimensional and unsteady flow simulations is possible, it is universally usable, and the developers continuously updates and upgrade the program incorporating new features every time. Of course, other models like FLOW2D, for example, are 12-40 times faster, and also can simulate 2D. However, they are not available freely. The available hydraulic models use the same governing equations, continuity and momentum equations. Differences in the simulation results are due to the modeler and how the results are interpreted. Therefore, HEC –RAS could safely be used for dam break studies.

3.4. Breaching mode

Dam failure may arise due to different reasons ranging from seepage, piping (internal erosion), overtopping due to insufficient spillway capacity and insufficient free board and to settlement due to slope slides on the upstream shells and liquefaction due to earthquakes. However, dam failure studies are conducted for two breach scenarios; overtopping and piping failure. As stated in the literature review section 2.3, the most possible cause of failure must be considered. In this study, only piping mode of failure was considered as justified in the same section in the literature review.

3.5. Model Development

Development of dam breach simulation using 2D- HEC–RAS model requires major data; Terrain/elevation data, hydraulic data/Manning's roughness coefficients, reservoir and dam profile data, breach parameters and hydrologic Data as a boundary conditions. These datasets were used in HEC–RAS and GIS environment to simulate the hypothetical breach.

3.5.1. Mesh Generation

2D mesh of size 20x 20 required to represent the downstream land surface were generated on the combined terrain data. The size is enough to represent most of the study area as it is flat flood plains and complied with the required computation time interval for stable solution. The mesh size also manually minimized at some locations where terrains are not flat. The storage area and the downstream area were connected using an inline structure (Gidabo dam) on HEC–RAS geometric data editor shown in Figure3. 5. The boundary was fixed according to a High flood level. The upstream boundaries were made at the reservoir extent. Refer Figure3. 5: UB-1, UB-2, UB-3 and UB-4 are upstream boundaries. DS-1 is the downstream boundary away from the settlement areas shown in the figure as blacken rectangles.

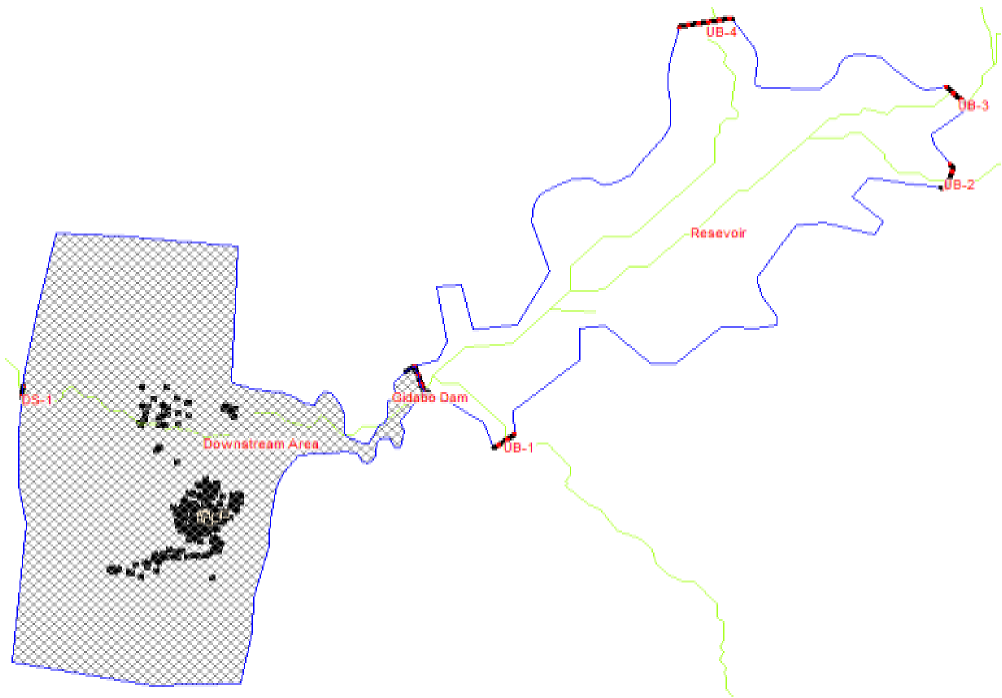

Figure3. 5: Study area: storage area and 2D downstream area. Note that the black spots represent current settlement areas

3.5.2. Manning's Roughness Coefficients

Manning's n values were used in the model to define roughness for the different land covers in the 2D area. The n -values were assigned by first defining land-use characteristics for common areas. This was done on high resolution rectified image produced from Smart GIS.

Each land-use characteristic was assigned an *n* -value based on Chow's (1959) published values for similar conditions; his description of different flood plains with their associated roughness value is provided in Appendix-A 7.The different land covers and their corresponding *n* values provided are shown in Figure3. 6. The roughness values associated with each land use with in the model area was then linked through land use terrain association in the geometric data editor on HEC-RAS. The ground photographs and tabular descriptions of the land uses with in the 2D area are placed in Appendix-A 5 and Appendix-A 6.

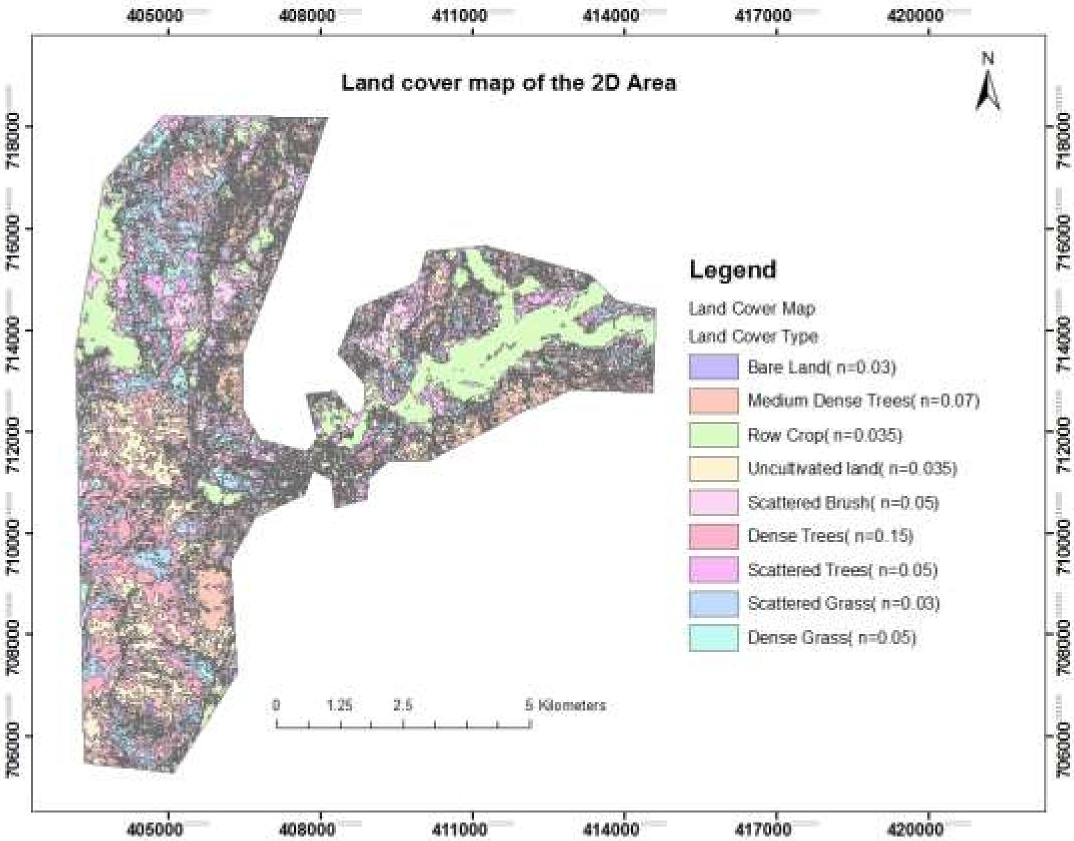

Figure3. 6: Lands cover classification with their roughness values.

3.5.3. Flow and Boundary Conditions

Flow hydrograph was used for each upstream boundary. Flow for different return period determined from a frequency analysis at the dam axis, shown in Appendix-A 8, were extrapolated based on the catchment area ratio for each upstream boundary locations. Figure3. 7 below show the upstream boundary locations, UB-1, UB-2, UB-3 and UB-4. These points are the junction between the storage area and the natural river. For each location the contributing catchment area was delineated on GIS environment. For example: Figure3. 8 show the extrapolated hydrograph at the boundary locations for 10000yr flow at dam axis.

Similar procedure was followed for other return periods. The normal depth close to the Lake Abaya was used as downstream boundary condition.

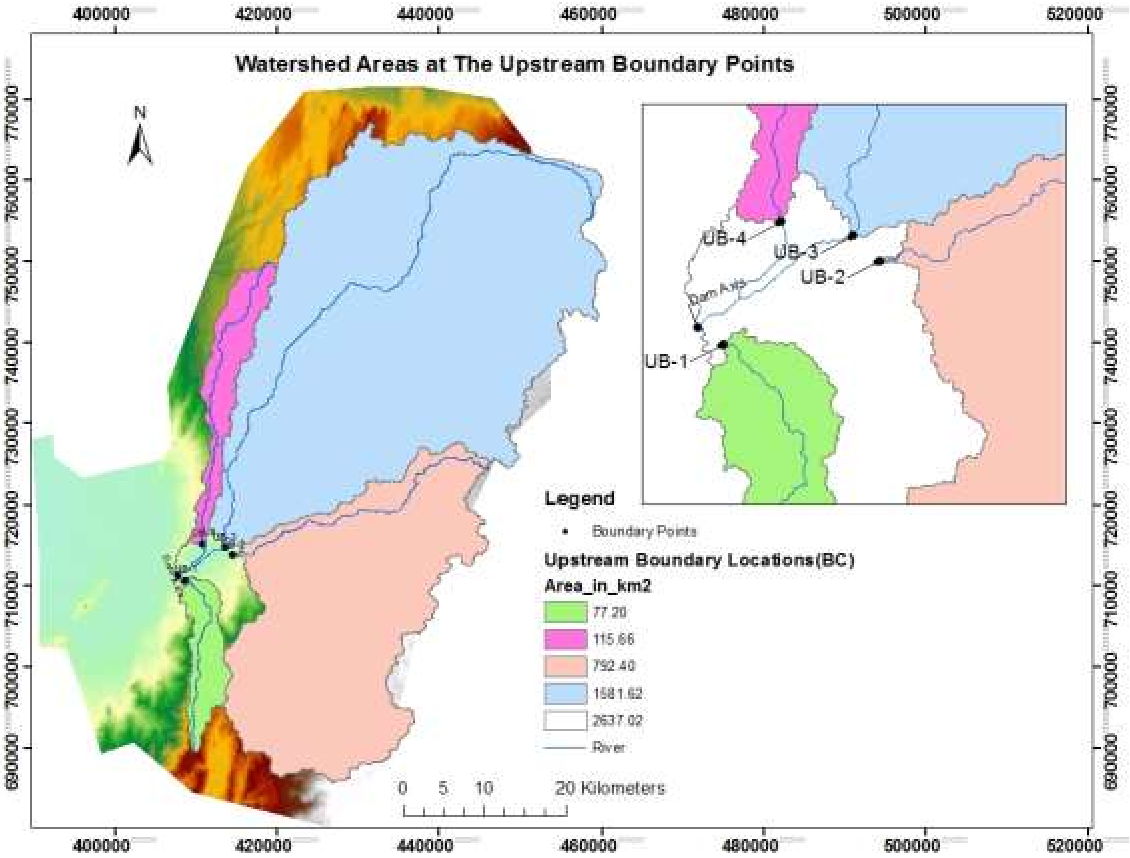

Figure3. 7: Catchment area at the dam axis and upstream boundary locations

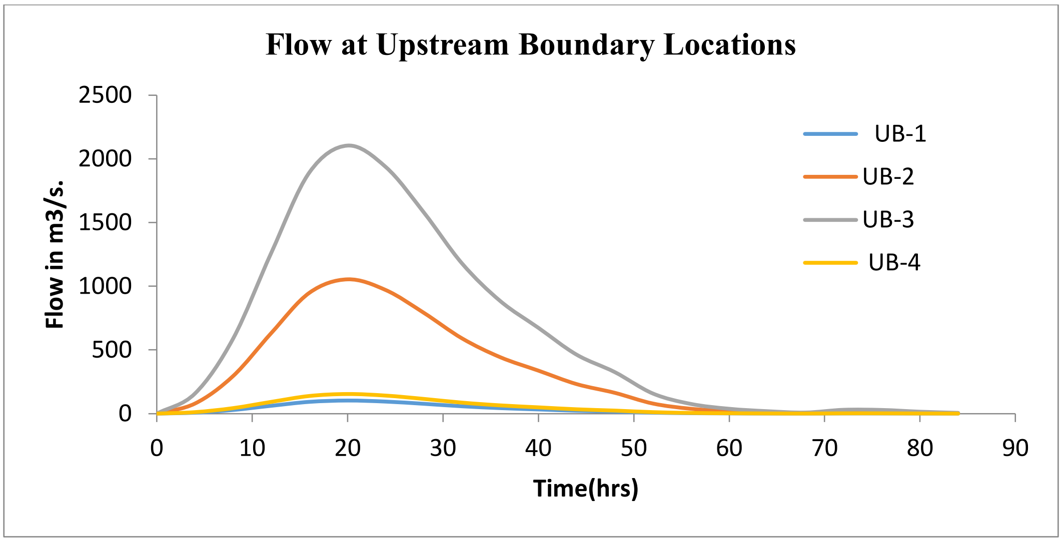

Figure3. 8: Flow hydrograph at upstream boundary locations

3.5.4. Dam-Breach Parameters

For piping failure mode the breaching parameters which include bottom width, side slopes and formation times were estimated using four techniques: MacDonald (1984), Froehlich (1995), Froehlich (2008) and Xu & Zhang (2009).

3.6. Flood-Inundation Mapping

Inundation mapping was done on Ras Mapper on the HEC RAS environment to identify the potential risk, safe settlement areas and alignment of preliminary protection works (levees). Water surface profile at location of interest that is at settlement areas were drawn on Ras Mapper. The outputs of the model were exported to GIS environment for further analysis and reporting purpose.

3.7. Sensitivity Analysis

Sensitivity analysis was performed in order to estimate the impact of varying the model parameters to the model results. These parameters include full formation time, breach depth, breach width, and breach side slope and roughness coefficient. The impact was studied by varying each factor by $\pm 20\%$ and 50% of the estimated values.

Result and Discussion

The following breach parameters were obtained (Figure4 1) for each methods implemented.

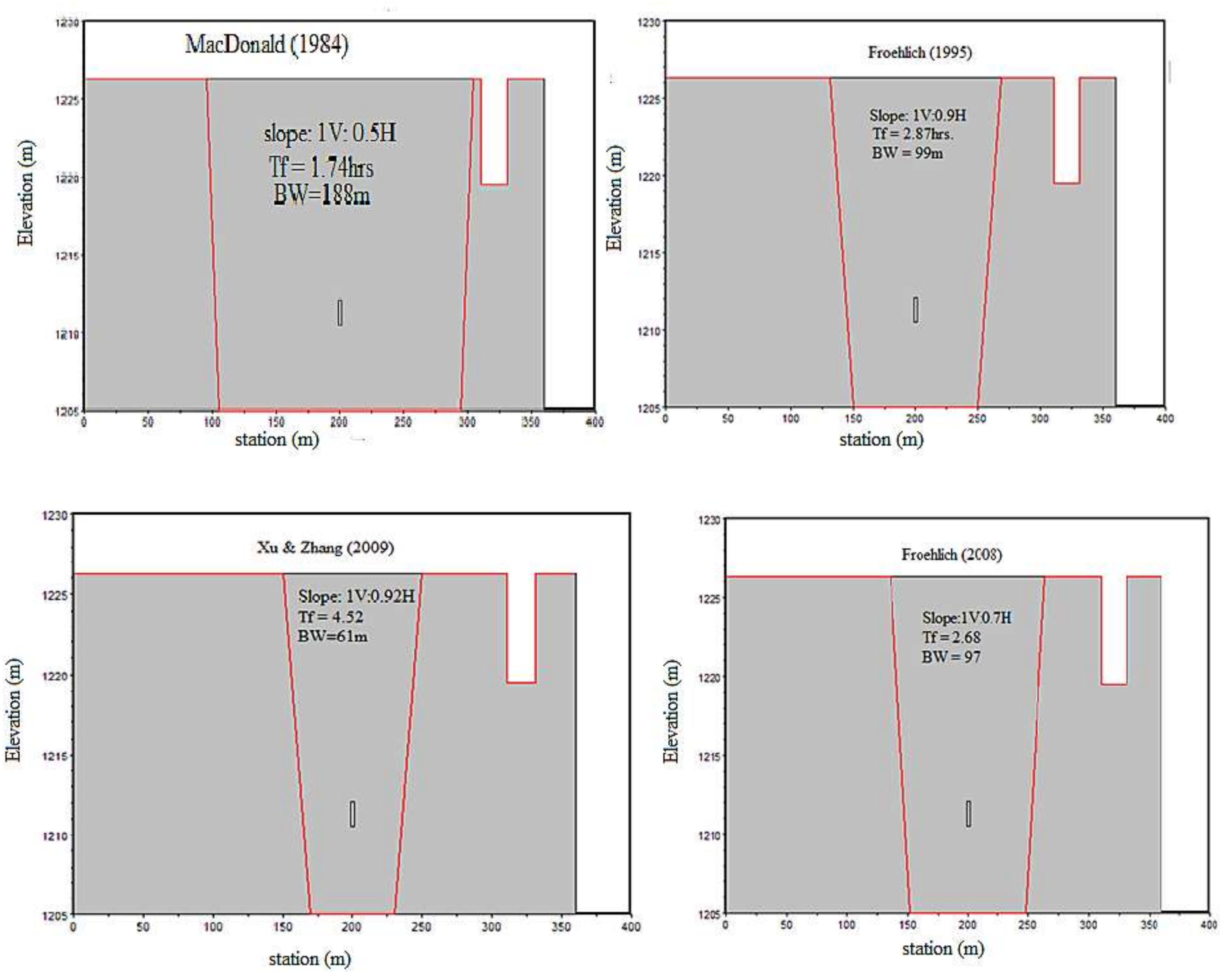

Figure4 1: Breach parameters as estimated by different methods. Note that: Tf =breach formation time, BW = final breach width

Since significant variations in the results were observed, one particular method should be selected according to the breach hydrograph. Figure4 2 shows the breach hydrograph estimates of each method. The breach from MacDonald estimation was the maximum, which was 9646.18m^3/s. 8715.1, 8715.1 and 7275.97 were maximum breach flow estimates based on Froehlich (1995, 2008) and Xu & Zhang (2009), respectively. The comparison made, for similar dam types, between observed flow from actual breach and estimated flows showed that all the breach estimates approximate larger flow hydrograph than the observed. The MacDonald's result was the largest. Though all the methods are based on regression of documented failed dams' data, difference exists on the number and type of dams studied. Froehlich in (1995) used 74 dams including earth fill, rock fill dams with a clay core. Again in 2008 revised his work with additional data. MacDonald (1984) being the oldest, however, considered 42 dams. Though Xu & Zhang (2009) examined 182 data sets, the final equations were developed using much lesser number of data set. Hence, Froehlich's (2008) estimation was taken to be appropriate for he used more data sets than the others, revised for second time which proves its refinement and mostly applied (universality) in determining breach parameters.

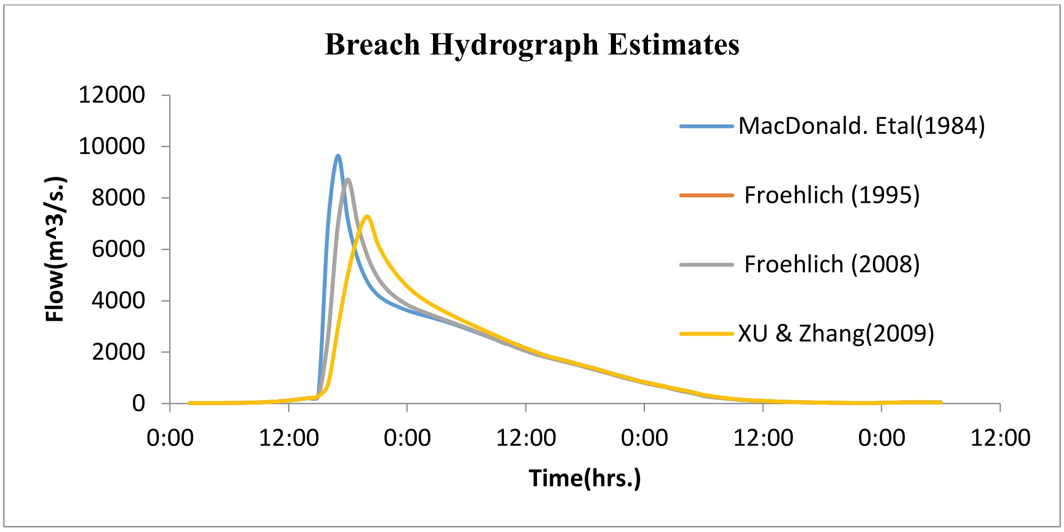

Figure4 2: Breach hydrograph based on the breach parameters

Each breach hydrograph was also routed on the downstream, Figure4 4 and Figure4 5 shows the flow hydrograph and flood depth profile right at the cross-section near the settlement area, 2.6km from the dam axis, Figure4 3.

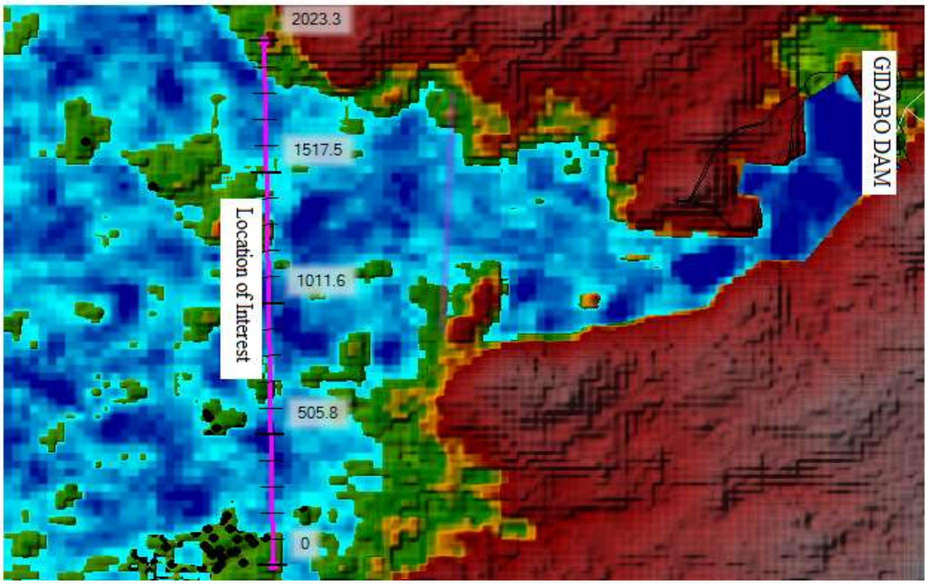

Figure4 3: Cross-section along the settlement areas, the dark spots represents residences

Attenuated flow of 181.1, 132.8, 92.3 and 53.0 m3/s were obtained for the corresponding breach hydrograph of MacDonald's (1984), Froehlich's (1995, 2008) and Xu & Zhang's (2009), respectively. The translation time of 5 minutes was obtained for each routed flow.

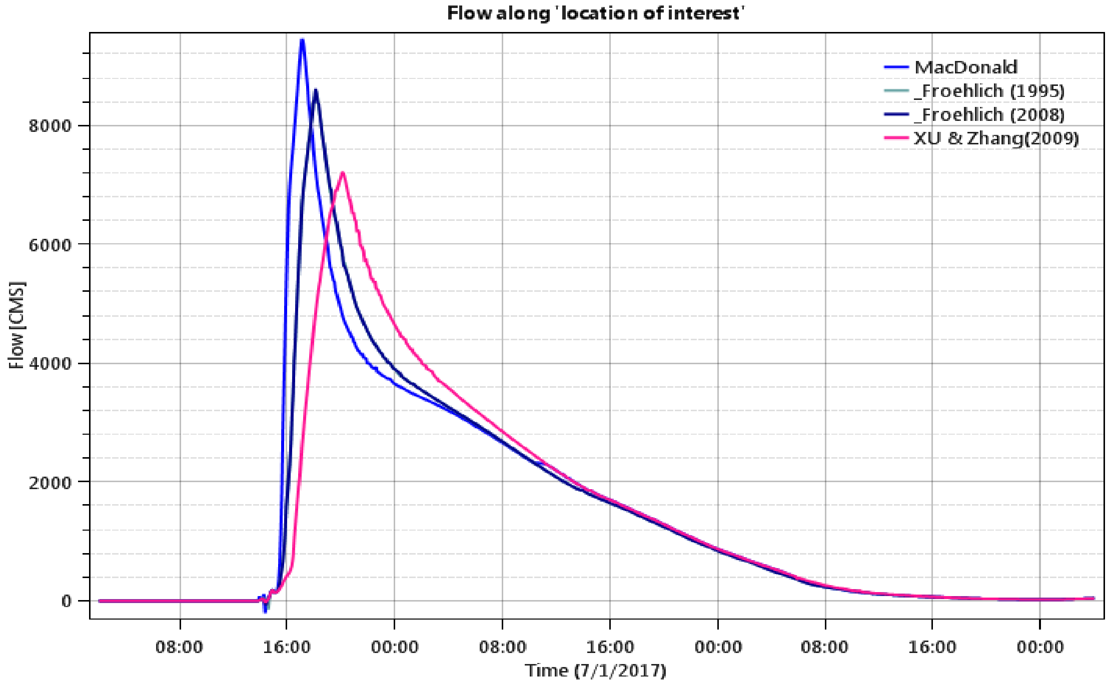

Figure4 4: Routed hydrograph at location of interest, close to settlement areas

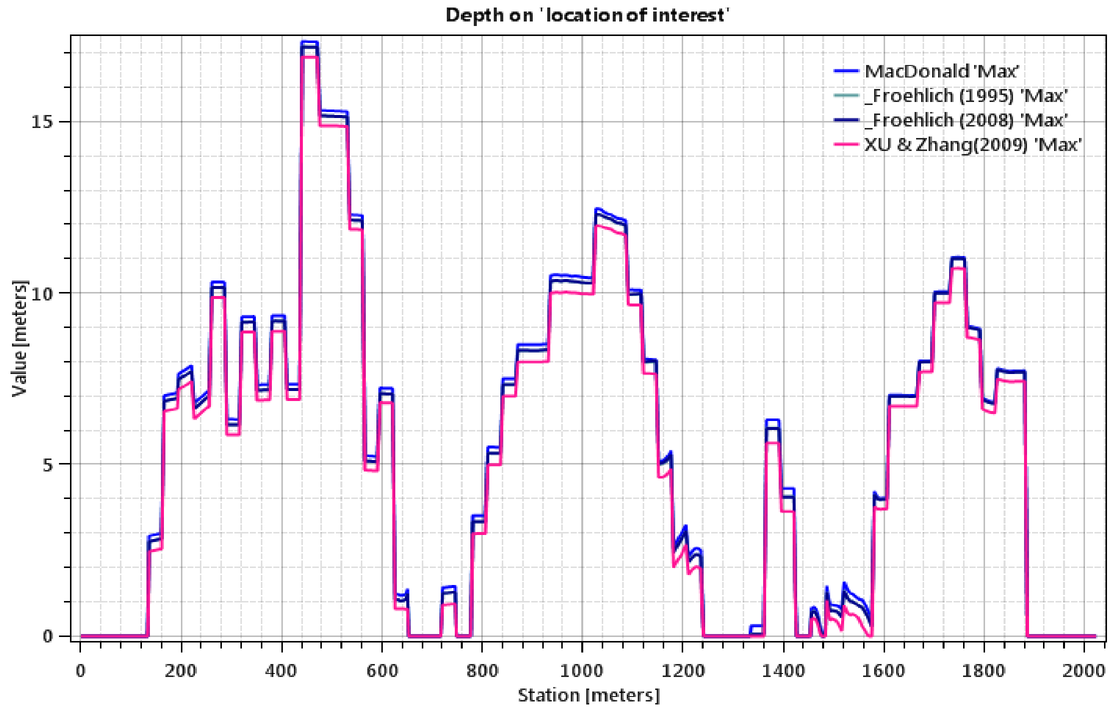

Figure4 5: Flood depth profile along a cross-section near settlement areas

The routed breach hydrograph was mapped on high resolution rectified image as shown on Figure4 6 so that the number of residences already at risk could easily be counted. Hence, of the total residences on the right bank looking in the direction of flow which only accounts 12% were totally with in the perimeter of the flood zone. However, residences on the left bank which totally accounts 88% of the total residence, 79% was found out to be at risk.

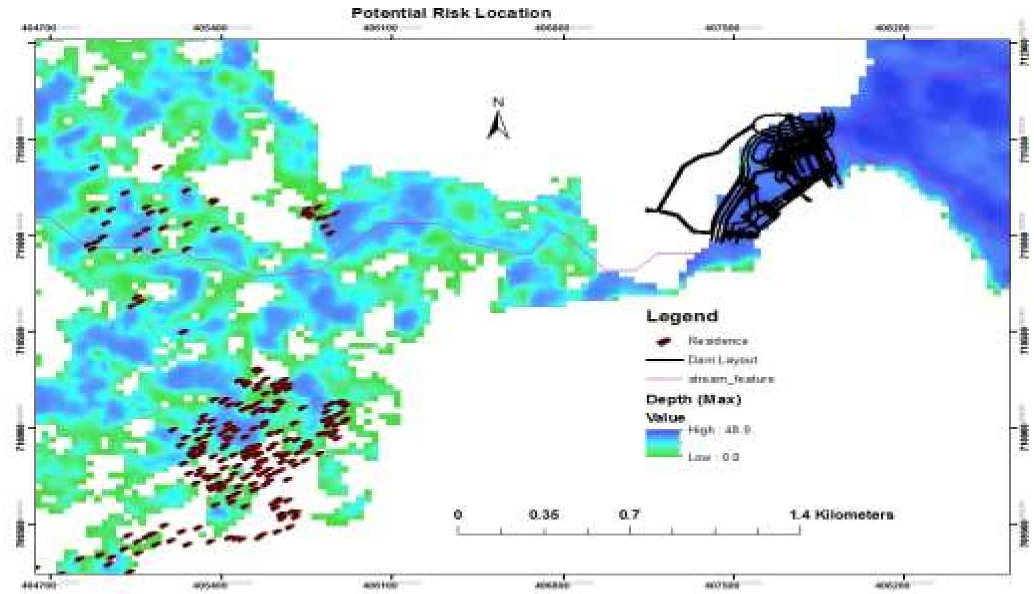

(a): Flood map

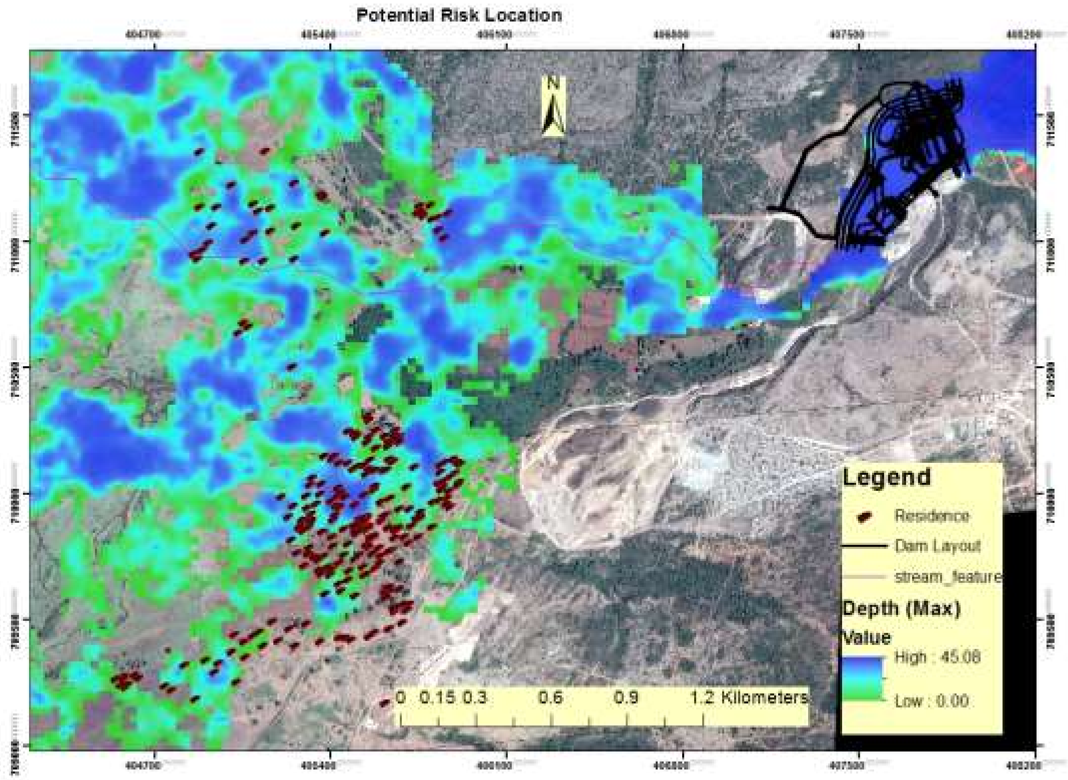

Figure4 6: Flood map (a) overlaid on high resolution satellite image (b)

Likewise unsafe settlement areas were identified following the perimeter of the mapped flood zone. Accordingly, the right bank was found out to be entirely unsafe not shown on the Figure4 7 whereas it is shown on the left bank. Fortunately, the numbers of residence on the right bank were minimal compared to the settlers on the left bank.

Figure4 7: Map showing polygon of unsafe settlement area

The potential risks could be reduced by devising flood protection works such as a dike, as one possible method. The preliminary alignment of the protection work is shown on the Figure4 8. Along this preliminary alignment the water surface elevation and terrain profile is shown on Figure4 9. Hence by having detailed design along this preliminary alignment the dam risk could be lessened by 2% or the people already at risk could be relocated to areas outside the perimeter shown in Figure4 7.

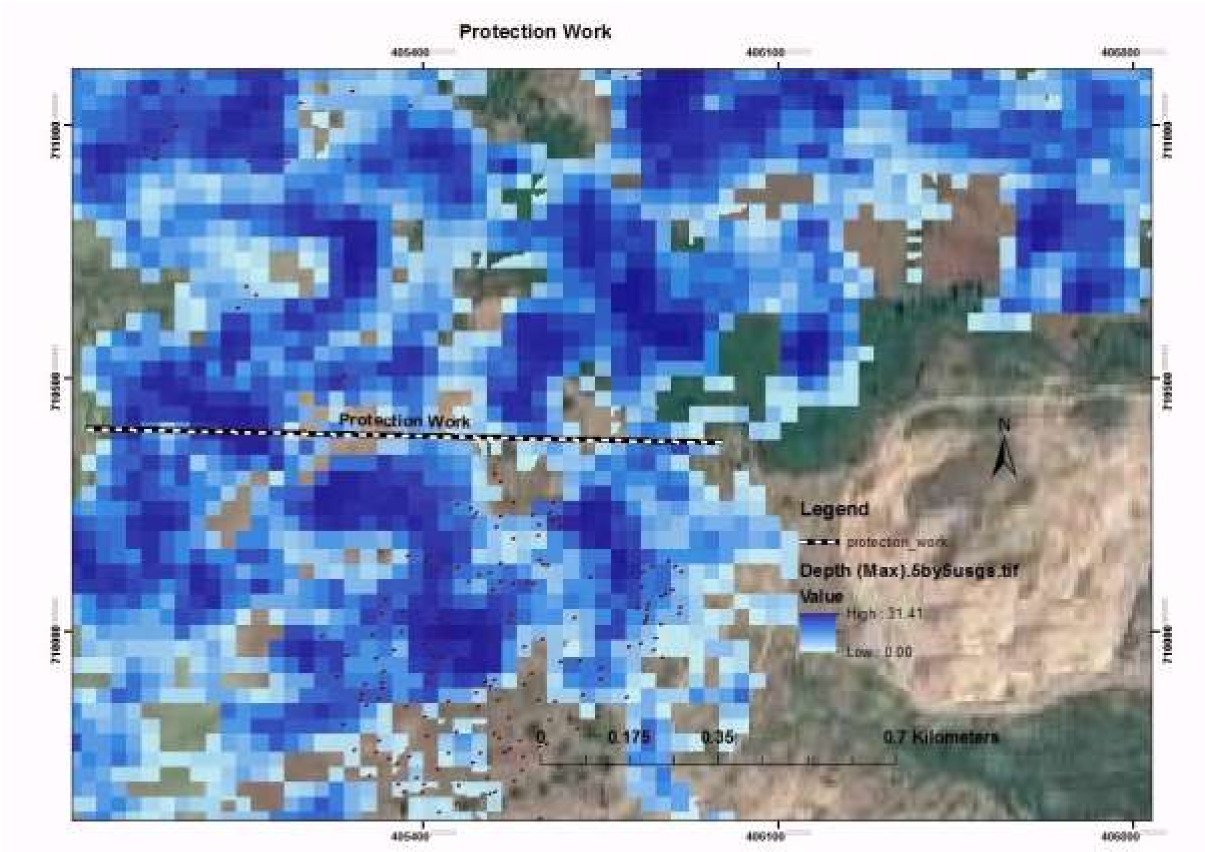

Figure4 8: Preliminary alignment of protection work

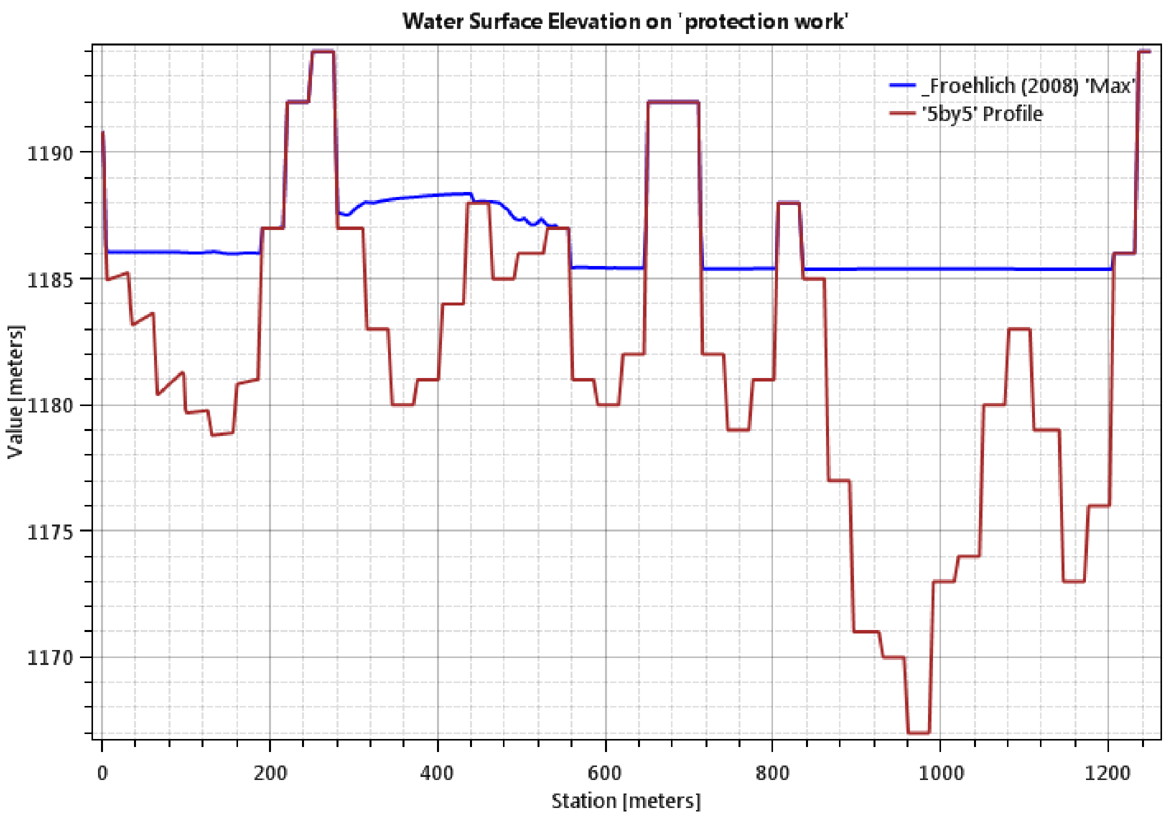

Figure4 9: Water surface profile and terrain profile along the axis of the protection work.

Sensitivity Analysis

Dam break inundation results are highly dependent on the breach parameters which are estimated based on a regression analysis and set of assumptions. Therefore it is imperative to analyze the impacts of varying these parameters on the results. These parameters include full formation time, breach height, breach width, and breach side slope. The result is also dependent on the manning roughness which is a dynamic flow parameter. Based on the simulated flow, the breach sensitivity analysis is summarized with figures in the subsequent paragraphs below. The impacts were analyzed at the location where residential exist, location of interest.

As shown in Figure4 10: Decreasing H_W by 20% and 50% resulted in an increase in the water surface elevation (WSE) by 1.33m and 1.40m, respectively. This increased the flooding risk on the left bank by 10%. Increasing H_W by 20%, however, decreases WSE by 1.10m. This caused the flooding risk to decrease by 26%. Increasing H_W by 50% increased WSE by 1.40m; the flooding risk increased by 10%.

As shown in Figure4 11: decreasing the slope by 20% and 50%, lowered the WSE by 0.86m and 0.87m, respectively; Whereas increasing the slope by the same factor, caused WSE to be dropped by 0.95m and raised by 1.65m. Changes of breach side slope by $\pm$ 20% and -50% reduced the flooding risk by 19%. However, a change of slope by +50% increased the flooding risk by 12%.

Likewise, referring Figure4 12; reducing the formation time by 20% and 50% resulted in a reduction of WSE by 0.96m and 1.85m, respectively. As a result, the flooding risk dropped by 22.5% on average. Increasing the full formation time by same factor increased the WSE by 1.41m and 1.21m, respectively. This change would increase the flooding risk by 12% on average.

Sensitivity analysis for various breach width also changed the result as shown in Figure4 13. Reducing the breach width by 20% increases the WSE only by 0.24m. Other change to B_W by the aforementioned factors reduces the WSE by an amount close to 1m. Flooding risk would be reduced by 22.5% when B_W was changed by +20% and +50%. For –50% changes, however, there would be 15% reduction and for -20% changes, it would remain the same, 79%.

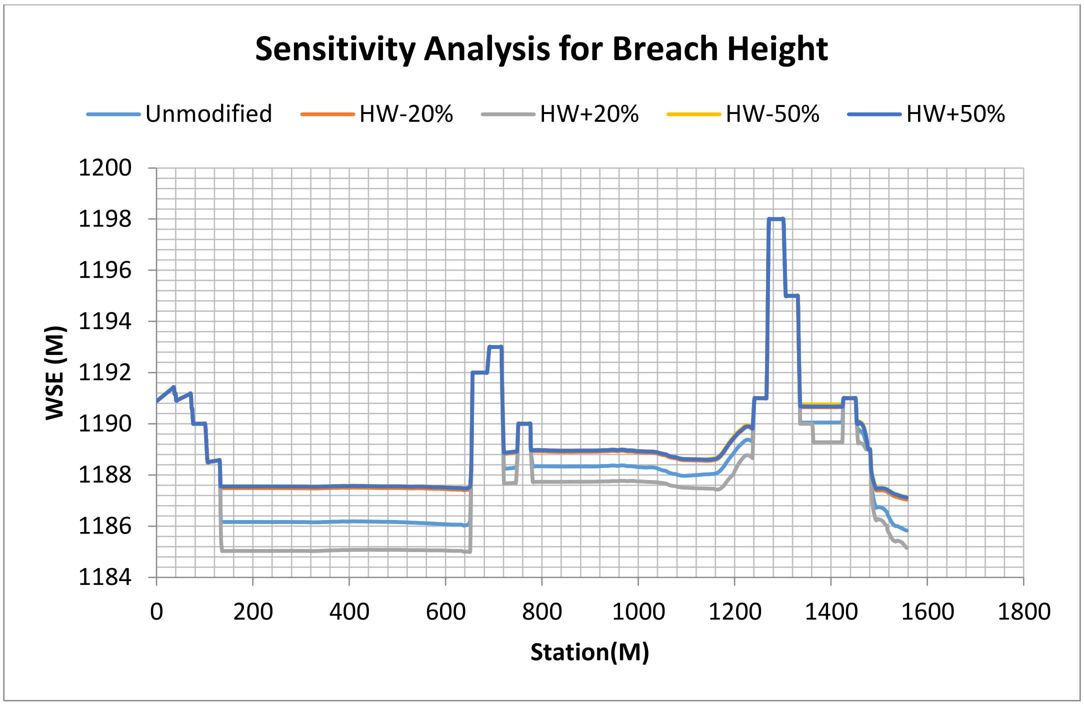

Figure4 10: sensitivity analysis for breach height.

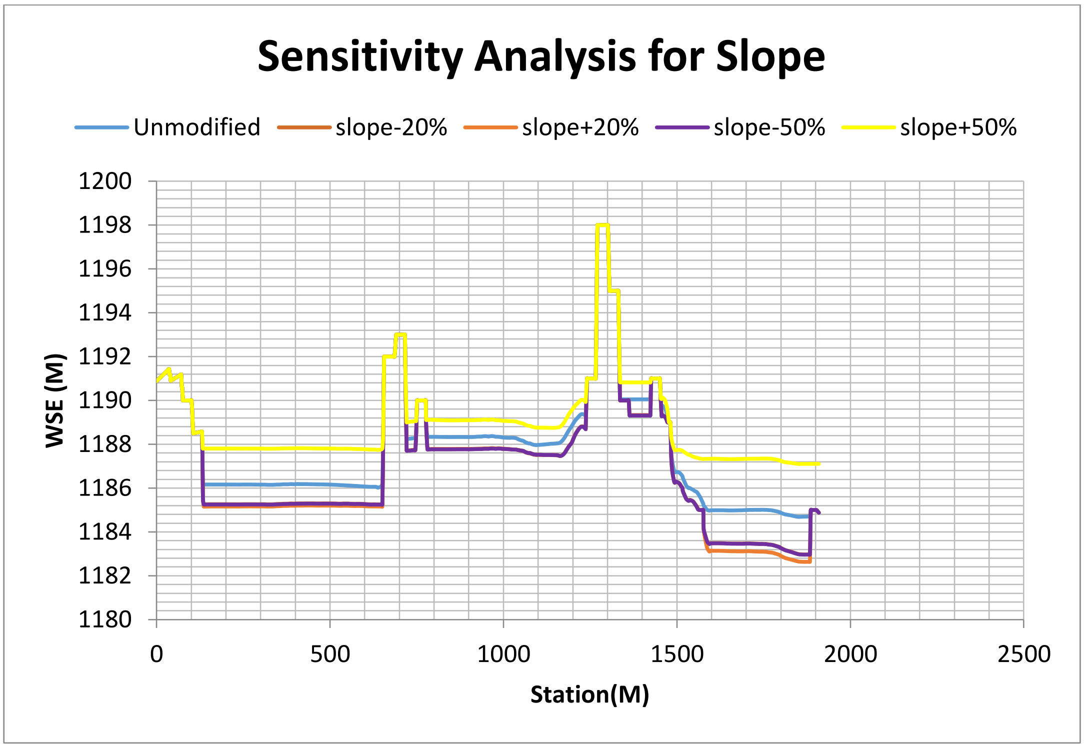

Figure4 11: sensitivity analysis for slope.

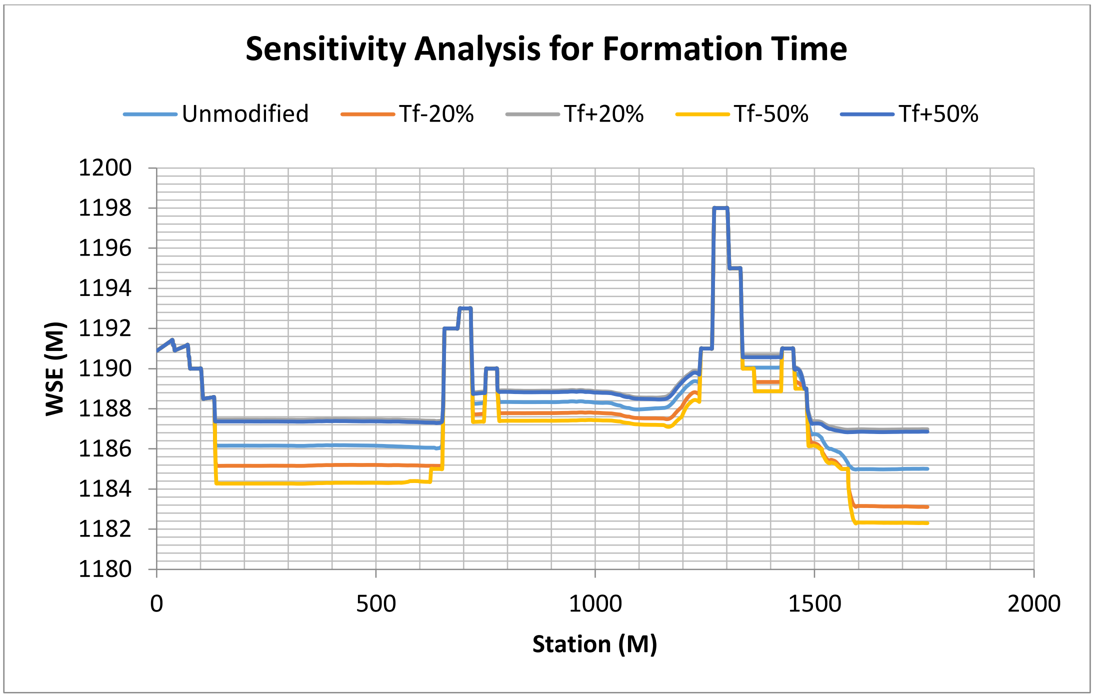

Figure4 12: Sensitivity analysis for full formation time.

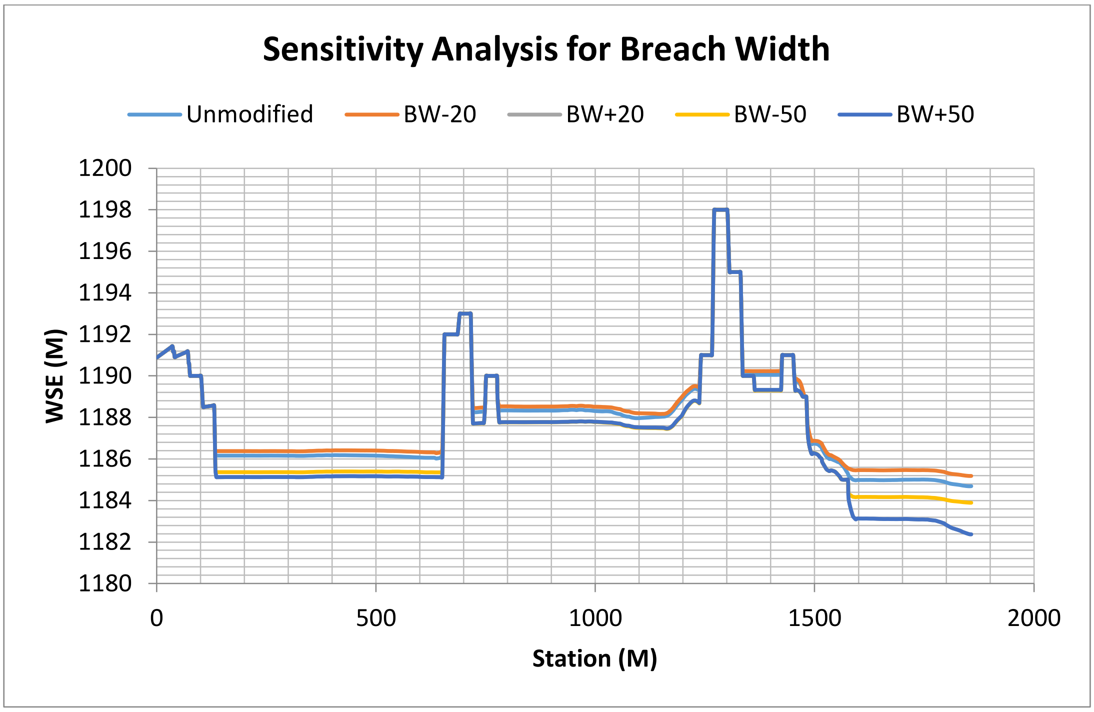

Figure4 13: Sensitivity analysis for full breach width.

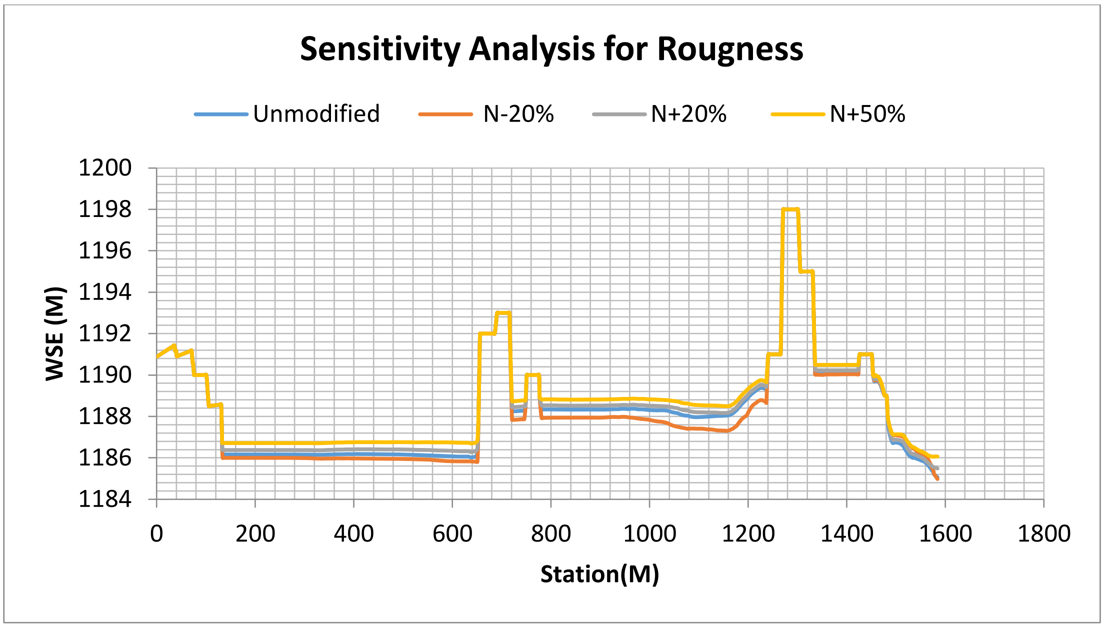

Figure4 14: Sensitivity analysis for manning roughness.

The result for sensitivity analysis for changes of roughness is shown in Figure4 14. Increasing roughness by 20 and 50 percent increased WSE by 0.24 and 0.60 m, respectively. This increased flooding risk only by 5%. Decreasing by 20% reduces the WSE by 0.21m, and the risk reduced by 6%.

In a nutshell, the sensitivity analysis performed for all the breach parameters and manning roughness showed that the flooding risk could be increased to 91%. This was determined for various changes of breach height, full formation time and side slope. Therefore, H_w could be regarded as the most sensitive parameter. T_f comes in second place. Slope, roughness and B_w could be placed in the next line in order of sensitiveness.

The initial breach height was made at the conduit level, which is the most reasonable breach initiation level. This is because conduit through embankment body creates weak alignment (at the contact between the conduit and the embankment material) and seepage specifically called contact seepage could be initiated most likely at this location than at any other within the dam. However, the sensitivity test indicated that higher breach initial locations would result in the worst inundation.

4. Conclusion

As the areas downstream of Gidabo dam is becoming a settlement area in recent years, dam breach flooding impact analysis become important. The study focused mainly on the downstream consequence of the dam in case of failure, determination of breach parameters, identifying residential already at risk and safe settlement area and determination of preliminary alignment of flood protection works.

The analysis was performed based on data which includes terrain, dam profile, land cover, and inflow hydrograph. Four well known breach parameter estimators were considered. Piping mode of failure with a number of flood scenarios was considered. Sensitivity analysis was performed for all breach parameters and manning roughness.

The results indicated a final breach width of 97m, side slopes 1V: 0.7H and breach formation time of 2.6h based on Froehlich's (2008) technique. With these breach parameters a peak discharge of 8700 m3/s would be expected. This discharge after full breach formation required a duration of 5 minutes to reach at the settlement area. The sensitivity test showed that H_w is the most sensitive parameter that could worsen the flooding impact by 12%. T_f comes in second place. Slope, roughness and B_w was found out to be in the next place in order of sensitiveness.

The entire settlement area of the right bank would be flooded and all would be at risk whereas 79% of the residences would be at risk on the left bank. The remaining 21% of the people were resided outside the risk zone. The flooding risk on the left bank could reach up to 91% as depicted from the sensitivity test results.

A structural flood mitigation measure like dike would reduce the dam risk and flood extent. A preliminary alignment of protection dike of about 1.25 km would reduce the potential risk to 2%.

5. Recommendation

In cases where a settlement area is prone to flood hazard a number of techniques can be applied to reduce the potential danger. However, only one measure that is dyke is considered and its alignment was decided in this paper. Future studies should assess other flood mitigation techniques and the one which is economically viable should be determined based on the results of this research.

The result of the study is useful for dam risk assessment and flood mitigation works. Therefore, stakeholders like ministry of water, irrigation and energy, land use planners of the nation should refer and use this research finding.

References

Ahmadisharaf, E., Kalyanapu, A. J., Thames, B. A. and Lillywhite, J. (2016) “A probabilistic framework for comparison of dam breach parameters and outflow hydrograph generated by different empirical prediction methods,” Environmental Modelling and Software. Elsevier Ltd, 86, pp. 248–263. doi: 10.1016/j.envsoft.2016.09.022.

Asnaashari, A., Eng, P., Engineer, H., Wood, K., Associates, L., Meredith, D., Ag, P., Manager, P., Wood, K., Associates, L., Scruton, M., Wood, K. and Associates, L. (2014) “DAM BREACH INUNDATION ANALYSIS USING HEC-RAS AND GIS TWO CASE STUDIES IN BRITISH COLUMBIA, CANADA,” (October).

Brunner, G. W. (2010) “HEC-RAS River Analysis System: User’s Manual (4.1),” (January).Brunner, G. W. (2015) “Tuflow vs Mike DHI products vs HEC-RAS 5,” in hdrologic/hydraulic modelr’s forum:Tuflow vs Mike DHI products vs HEC-RAS 5. Available at: HTTP://hecrasmodel.blogspot.com/2015/12/HEC-RAS-50-VERSUS-TUFLOW-VERSUS-MIKE21.HTML, June 8,2017 @07:05AM.

Changzhi, L., Hong, W., Zhixue, C., Yongfeng, Y., Zhengfu, R. and Mike, C. (2014) “Dam Break Flood Risk Assessment for Laiyang City,” 4, pp. 189–199. doi: 10.17265/2328-2193/2014.04.001.

Coon, W. F. (1997) Estimation of roughness coefficients for natural stream channels with vegetated banks, U.S. Geological Survey water-supply paper.

David, S. B., Loren, R. A., A., Terry, F. G. 1998. and Al, E. (1998) THE PRACTICE OF DAM SAFETY RISK ASSESSMENT AND MANAGEMENT: ITS ROOTS, ITS BRANCHES, AND ITS FRUIT. Presented at the Eighteenth USCOLD Annual Meeting and Lecture,Buffalo, New York.

FERC (2014) “FERC Engineering Guidelines Risk-Informed Decision Making,” chapter R21, Dam Breach Analysis.

Gallegos, H. A., Schubert, J. E., Sanders, B. F. and Al, E. (2009) “Two-dimensional, high-resolution modeling of urban dam-break flooding: A case study of Baldwin Hills, California,” Advances in Water Resources. Elsevier Ltd, 32(8), pp. 1323–1335. doi: 10.1016/j.advwatres.2009.05.008.

Gee, D. M. (2008) “comparison of dam breach parameter estimators,” Senior Hydraulic Engineer, Corps of Engineers Hydrologic Engineering Center, 609 2nd St., Davis, CA 95616; email: michael.gee@usace.army.mil.

Kulkarni, S. R., Ukarande, S. K., Jagtap, S. A. and Al, E. (2016) “Dam Break Analysis - A Case Study,” 6890(5), pp. 207–209.

Lejissa, H. (2015) Dam Breach Modelling and Downstream Risk Analysis (For Arjo-Dedessa Dam). Addis Ababa University.

McCuen, R. H. (2017) “Risk Assessment in Dam Safety Analysis Author (s): Richard H . McCuen Source : Journal of the Washington Academy of Sciences , Vol . 69 , No . 4 (December , 1979), Published by : Washington Academy of Sciences Stable URL : http://www.jstor.org/stable/,” 69(4), pp. 146–150.

Reinaldo, G. (2015) Dam-Break-and-Tailings-Dam-Breach-Flooding-Simulations -using SMS.

Sanders, B. F. (2007) “Evaluation of on-line DEMs for flood inundation modeling,” Advances in Water Resources, 30(8), pp. 1831–1843. doi: 10.1016/j.advwatres.2007.02.005.

Shivers, M. J., Smith, S. J., Grout, T. S. and, Lewis, J. M. and Al, E. (2015) “Dam-Breach Analysis and Flood-Inundation Mapping for Selected Dams in Oklahoma City , Oklahoma , and near Atoka , Oklahoma Scientific Investigations Report 2015 – 5052.”

Xiong, Y. (2011) “A Dam Break Analysis Using HEC-RAS,” Journal of Water Resource and Protection, 3(June), pp. 370–379. doi: 10.4236/jwarp.2011.36047.

Appendices

1. Xu and Zhang (2009):

$$\frac{B_{avg}}{h_b} = 0.787\left(\frac{h_d}{h_r}\right)^{0.133}\left(\frac{{V_w}^{1/3}}{h_w}\right)^{0.133} e^{B_3}$$

Where: B_{avg}= average breach width (m)

V_w= reservoir volume at the time of failure (m^3)

h_b=height of the final breach (m)

h_d=height of the dam (m)

h_r=15m reference height distinguishing large dams from small dams

h_w=height of the water above the breach bottom elevation at time of breach (m)

$B_3=b_3+b_4+b_5$, coefficient that is function of dam property

b_3=-0.041, 0.026, and -0.226 for dams with core walls, concrete faced, homogenous/zoned

b_4=0.149, -0.389 for overtopping and piping respectively

b_5=0.291,-0.14, and -0.391 for high, medium and low dam erodibility

The Xu and Zhang do not provide estimates for side slope directly. Instead they provide an equation to estimate the top width of the breach, which can then be used with average breach width, to compute the corresponding side slopes here is there equation for the breach

$$\frac{B_t}{h_b} = 1.062\left(\frac{h_d}{h_r}\right)^{0.092}\left(\frac{{V_w}^{1/3}}{h_w}\right)^{0.508} e^{B_2}$$

Where: B_t=breach top width (m)

$B_2= b_3+b_4+b_5$, coefficient that is function of dam property

b_3=-0.061, 0.088, and -0.089 for dams with core walls, concrete faced, homogenous/zoned

b_4=0.299, -0.239 for overtopping and piping respectively

b_5=0.411,-0.062, and -0.289 for high, medium and low dam erodibility

Breach side slopes can be computed with the following equation:

$$z = \frac{B_t - B_w}{h_b}$$

Appendix-A 1: Xu and Zhang's regression equation for Breach width and slope

Xu and Zhang (2009) continued

$$\frac{T_f}{T_r} = 0.304\left(\frac{h_d}{h_r}\right)^{0.707}\left(\frac{V_w{}^{1/3}}{h_w}\right)^{1.228} e^{B_3}$$

Where: T_f=breach formation time (hrs.)

T_r=1 hour (unit duration)

V_w= reservoir volume at the time of failure (m^3)

h_d=height of the dam (m)

h_b=height of the final breach (m)

$B_3=b_3+b_4+b_5$, coefficient that is function of dam property

b_3=-0.327, -0.674, and -0.189 for dams with core walls, concrete faced, homogenous/zoned

b_4=- 0.579, -0.611 for overtopping and piping respectively

b_5= -1.205,-0.564, and -0.579 for high, medium and low dam erodibility

Appendix-A 2: Xu and Zhang's regression equations for slope and full formation time

2. Federal Agency Guidelines

Dam Type	Average Breach Width B_{ave}	Horizontal Components of Breach Side Slope(H) H:1V	Failure Time T_f (Hrs.)	Agency
Earthen/Rockfill	(0.5 to 3.0) x HD (0.5 to 5.0) x HD (1.0 to 5.0) x HD (2.0 to 5.0) x HD	0 to 1.0 0 to 1.0 0 to 1.0 0 to 1.0 (slightly larger)	0.5 to 4.0 0.1 to 4.0 0.1 to 1.0 0.1 to 1.0	USACE (1980) USACE (2007) FERC (1988) NWS (FREAD, 2006)
Concrete Gravity	Multiple Monoliths Usually ≤ 0.5 L Usually ≤ 0.5 L	Vertical Vertical Vertical	0.1 to 0.5 0.1 to 0.3 0.1 to 0.2	USACE (2007) FERC NWS
Concrete Arch	entire dam (0.8x L) to L entire dam (0.8x L) to L	valley wall slope 0 to valley walls 0 to valley walls 0 to valley walls	≤ 0.1 ≤ 0.1 ≤ 0.1 ≤ 0.1	USACE (1980) USACE (2007) FERC NWS
Slag/ Refuse	(0.8x L) to L (0.8x L) to L	1.0 to 2.0	0.1 to 0.3 ≤ 0.1	FERC NWS
Where HD = Height of The Dam. L= Length of The Dam Crest				

Appendix-A 3: Range of Possible Values for Breach Characteristics (source: USACE, 2014. "Using HEC-RAS for dam break studies," page-8)

3. Dam profile

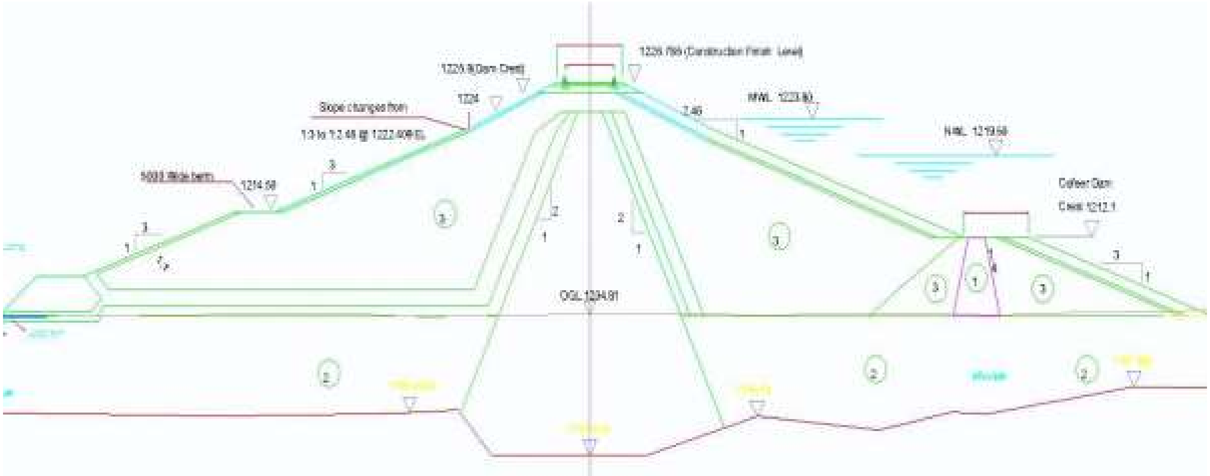

Appendix-A 4: Dam profile *(source: WWDSE)*

4. Roughness Values determination

land cover for grid code101430,n=0.15

: land cover for grid code103834,n=0.05

land cover for grid code103869, n=0.03

land cover for grid code16895,n =0.03

Appendix-A 5: photographs showing different land cover in the study area

Roughness value determination continued

land cover for grid code84140, n=0.03/0.035

land cover for grid code53118, n=0.07

land cover for grid code95548, n=0.05

land cover for grid code68118, n=0.035

Appendix-A 6: photographs showing different land cover in the study area

5. Chow's (1959) Roughness coefficient value

Hydraulic Roughness (Manning's N)			
Values of Natural Channels and Floodplains			
Channel	Minimum	Normal	Maximum
A. Minor streams (top width at flood stage less than 100 feet)			
1. Streams on plain			
a. Clean, straight, full stage, no rifts or deep pools	0.025	0.03	0.033
b. Same as above, but more stones and weeds	0.03	0.035	0.04
c. Clean, winding, some pools and shoals	0.033	0.04	0.045
d. Same as above, but some weeds and stones	0.035	0.045	0.05
e. Same as above, lower stages, irregular slopes and sections with more ineffective flow area	0.04	0.048	0.055
f. Same as d, but more stones	0.045	0.05	0.06
g. Sluggish reaches, weedy, deep pools	0.050	0.070	0.080
2. Mountain streams, no vegetation in channel, banks usually steep, trees and brush along banks submerged at high stages			
a. Bottom: gravels, cobbles, and few boulders	0.03	0.04	0.05
b. Bottom: cobbles with large boulders	0.04	0.05	0.07
B. Floodplains			
1. Pasture, no brush			
a. Short grass	0.025	0.03	0.035
b. High grass	0.03	0.035	0.05
2. Cultivated areas			
a. No crop	0.025	0.035	0.045
b. Mature row crops	0.025	0.035	0.045
c. Mature field crops	0.03	0.04	0.05
3. Brush			
a. Scattered brush, heavy weeds	0.035	0.05	0.07
b. Light brush and trees, in winter	0.035	0.05	0.06
c. Light brush and trees, in summer	0.04	0.06	0.08
d. Medium to dense brush, in winter	0.045	0.07	0.11
e. Medium to dense brush, in summer	0.07	0.1	0.16
4. Trees			
a. Dense willows, summer, straight	0.11	0.15	0.2
b. Cleared land with tree stumps, no sprouts	0.03	0.04	0.05
c. Same as above, but with heavy growth of sprouts	0.05	0.06	0.08
d. Heavy stand of timber, a few down trees, little undergrowth, flood stage below branches	0.08	0.1	0.12
e. Same as above, but with flood stage reaching branches	0.1	0.12	0.16

Appendix-A 7: Hydraulic Roughness values for natural channels and flood plains, Chow (1959).

6. Secondary Hydrologic data determined through frequency analysis at the dam axis.

Frequency Flood (m3/s)				
Time (hrs.)	**2 Year**	**100 year**	**10000 year**	**PMF**
0	0	0	0	0
3.4	7	32.11	134.8	263.09
6.9	26	119.87	503.27	982.14
10.3	55.7	256.86	1078.43	2104.69
13.8	83.5	385.3	1617.64	3157.04
17.2	92.9	428.11	1793.36	3507.52
20.7	85.4	393.86	1653.59	3227.2
24.1	69.6	321.08	1348.03	2630.87
27.6	52	239.74	1006.53	1964.38
31	39	179.8	753.9	1473.29
34.5	29.7	136.99	575.16	1122.5
43.1	20.4	94.18	395.42	771.72
47.4	14.4	66.36	278.59	543.71
50.7	7	32.11	134.8	263.09
60.3	3.3	15.41	64.71	126.28
69	1.7	7.71	32.35	63.14
77.6	0.8	3.85	16.18	31.51
86.2	0.4	1.71	7.19	14.03

Appendix-A 8: Flow data at the dam axis (*source*: WWDSE)